STOCHASTIC MODELING AND QUANTIFICATION OF MULTIPATH ERROR IN STATIC GNSS OBSERVATIONS USING RTKLIB

BY

NNAMDI SUCCESS UGOCHUKWU

ENV2002788

DEPARTMENT OF GEOMATICS

UNIVERSITY OF BENIN

BENIN CITY, NIGERIA

P.M.B 1154

SUBMITTED IN PARTIAL FULFILMENT OF THE REQUIREMENTS FOR THE AWARD OF A BACHELOR OF SCIENCES {BSCGEM - B.SC. GEOMATICS} DEGREE, IN THE FACULTY OF ENVIRONMENTAL SCIENCES, UNIVERSITY OF BENIN, BENIN CITY, EDO STATE, NIGERIA

APRIL, 2025

STOCHASTIC MODELING AND QUANTIFICATION OF MULTIPATH ERROR IN STATIC GNSS OBSERVATIONS USING RTKLIB

A PROJECT SUBMITTED

BY

NNAMDI SUCCESS UGOCHUKWU

ENV2002788

SUBMITTED IN PARTIAL FULFILMENT OF THE REQUIREMENTS FOR THE AWARD OF A BACHELOR OF SCIENCES {BSCGEM - B.SC. GEOMATICS} DEGREE, IN THE FACULTY OF ENVIRONMENTAL SCIENCES, UNIVERSITY OF BENIN, BENIN CITY, EDO STATE, NIGERIA.

APRIL, 2025

CERTIFICATION

This is to certify that this project was carried out by **NNAMDI SUCCESS UGOCHUKWU** with Matriculation Number: **ENV2002788** of the Department of Surveying and Geoinformatics, Faculty of Environmental Sciences, University of Benin, Edo State, Nigeria.

SUPERVISOR Date…….

Surv. Dr. G.O NWODO

HEAD OF DEPARTMENT Date……..

Surv. Dr. S.O. Oladosu

EXTERNAL SUPERVISOR Date…….

DEDICATION

I humbly dedicate this project to Almighty God for His grace upon my life, and to my father and mother Mr & Mrs Henry Nnamdi for the path they laid out for me. May God continue to bless them. Amen.

ACKNOWLEDGEMENT

With a heart of gratitude, I return all glory, honor, and praise to God Almighty for granting me the strenght to embark on this B.Sc. programme and successfully complete it.

I appreciate my supervisor, Surv. Dr. G.O NWODO who took time out of his busy academic and administration engagements to correct and contribute meaningfully to my research. His encouragement and input in all aspects have given this project a worthy facelift. God bless you and your family.

I extend my appreciation to my loving Parent, Mr & Mrs Henry Nnamdi for their unwavering support both morally and financially which has helped me thus far in life. I also extend my gratitude to my Friend Esade Hannah for all of her kind gestures. May God reward you all greatly.

I also want to acknowledge my pastors Moses Edomwonyi, Theophilus Ugiagbe who stood strong in encouragement with me, and for their prayers and moral support during this journey.

I would like to thank the staff and management of the Department of Surveying and Geoinformatics at the University of Benin for their advice and guidance: Engr. Surv. Prof. Raphael Ehigiator, Surv. Dr. Nwodo Geoffrey, Surv. Dr. S.O Oladosu, Engr. Dr. Okonofua Solomon, Surv. M. Ekun, Surv. Dr Ojo Peter, Surv. Dr. Odunmosu, Surv. Tijani Mohammed, Engr. Mabel Alenkhe, Engr Kelly Iginidu and other staff members of the department. May God be gracious to you all.

ABSTACT

This study presents the stochastic modeling and quantification of multipath error in static Global Navigation Satellite System (GNSS) observations processed using RTKLIB. Multipath remains a major source of positioning inaccuracy, particularly in obstructed environments. The research statistically characterizes multipath and evaluates its contribution to overall observation uncertainty through a data-driven modeling approach.

Static GNSS data were collected under two contrasting conditions, an open-sky environment and a multipath-prone site, using Tersus GNSS receivers. Pseudorange residuals, satellite elevation angles, and carrier-to-noise ratios (C/N_0) were extracted from RTKLIB output files and filtered with a Python-based parser to ensure consistency. The cleaned datasets were then used to develop a stochastic model expressing observation variance as a function of satellite elevation and signal strength. Parameter estimation employed least squares and non-negative least squares (NNLS) regression to ensure physically meaningful variance predictions.

Results from the open-sky dataset revealed a baseline variance (σ_0^2) of 0.000000 m² and an elevation-dependent coefficient $a_1 = 1.6456$, indicating stable, low-noise observations. The multipath-prone site exhibited a much larger baseline variance ($\sigma_0^2 = 142.97$ m²) and stronger elevation and signal dependency ($a_1 = 10.063$, $a_2 = 4.79 \times 10^8$), reflecting severe distortion from signal reflection. About **25%** of pseudorange variance in open-sky conditions was explained by elevation and C/N_0, slightly less under multipath due to irregular reflections.

Multipath variances showed heavy-tailed distributions, with 95th-percentile values of 2,726 m² (≈52.2 m) under multipath and 63.6 m² (≈8.0 m) in open-sky conditions. Certain PRNs were consistently more affected, confirming the directional dependency of multipath. The developed stochastic model effectively relates satellite geometry and signal strength to pseudorange precision, providing a reliable framework for improving GNSS accuracy in multipath environments

TABLE OF CONTENTS

LIST OF TABLES

LIST OF FIGURES

CHAPTER ONE

INTRODUCTION

1.1 Background of the Study

Global Navigation Satellite Systems (GNSS) have become one of the most useful tools in modern surveying, mapping, navigation, and engineering. Today, many activities from land surveys to road design, environmental monitoring, and autonomous navigation depend on the ability of GNSS to provide accurate and reliable positioning data anywhere in the world.

However, the accuracy of GNSS observations can be influenced by several factors, including satellite geometry, atmospheric delays, signal strength, receiver quality, and surrounding environmental conditions. Among these, multipath is one of the most common and troublesome sources of error. Multipath occurs when GNSS signals reflect off nearby surfaces such as buildings, vehicles, or tree canopies before reaching the receiver's antenna. These reflected signals interfere with the direct ones, causing errors in the measured pseudorange or carrier phase and, ultimately, reducing the accuracy of the computed position.

Under open-sky conditions, GNSS measurements are generally stable and predictable because signal interference is minimal. But in environments where reflective surfaces are common, such as within the University of Benin campus multipath becomes more pronounced. Traditional data processing software usually applies simple weighting models that assume all observations are equally reliable or only depend on satellite elevation angles. Unfortunately, these assumptions are not always accurate in real-world conditions where SNR (Signal-to-Noise Ratio) and environmental factors vary widely.

To get better positioning results, it is important to develop a stochastic model that correctly represents how observation errors behave in both open-sky and multipath-prone areas. A stochastic model helps determine the correct weights to assign to different satellite observations based on their quality. With such a model, GNSS processing software can produce results that are more accurate, realistic, and consistent.

This research focuses on developing and testing such a stochastic model using static GNSS data collected around the University of Benin. The study will also assess how multipath affects GNSS positioning in different parts of the campus and how these errors vary spatially. The open-source software RTKLIB will be used for processing the GNSS data because of its flexibility, accessibility, and ability to provide detailed raw data for analysis.

The emergence of Global Navigation Satellite Systems (GNSS), such as the Global Positioning System (GPS), has significantly transformed modern navigation, surveying, mapping, and geospatial data collection. These systems are widely used due to their ability to provide precise location information in real time, enabling applications across fields such as land surveying.

GNSS positioning works by measuring the time it takes for signals transmitted from multiple satellites to reach a receiver on the Earth's surface. Based on the timing and known positions of these satellites, the receiver can compute its location through a process called trilateration. While GNSS systems are designed to provide highly accurate positioning information, the reliability and accuracy of the position data can be significantly affected by several types of errors. Among these errors, multipath interference remains one of the most complex and persistent challenges, especially in built-up or obstructed environments. The University of Benin campuses: Ugbowo (main) and Ekehuan have academic and administrative buildings, open lawns, vegetation, wooded

areas, and metallic infrastructure. These features create conditions conducive to multipath propagation, GNSS signal obstruction and multipath effects that fall somewhere between ideal open-sky conditions and tightly built urban canyons (University of Benin, 2024; Akhigbe et al., 2023).

Multipath occurs when satellite signals reach the GNSS receiver via multiple paths a direct path and one or more reflected paths. These reflections often result from nearby structures such as buildings, metal surfaces, or natural features like trees and bodies of water. Since reflected signals travel longer distances than direct signals, they arrive at the receiver with a time delay, leading to inaccurate distance measurements and, ultimately, erroneous position calculations. Despite advances in GNSS receiver technology and satellite signal processing, multipath errors remain difficult to eliminate entirely because they are site-specific and dynamic. The severity of multipath effects are often sinusoidal in phase residuals, receiver sensitivity, satellite geometry, and the nature of the reflecting surfaces (Marios Smyrnaios et al., 2013). In high-precision applications like engineering and cadastral surveying, even small positioning errors caused by multipath can result in significant discrepancies in measurements and project outcomes. Therefore, understanding and mitigating multipath effects is essential to ensure data integrity and positioning accuracy. For instance, surveyors operating near tall structures or under tree canopies within the university premises may experience degraded GNSS accuracy due to signal reflection and scattering.

Additionally, areas with narrow passages between buildings or walls can create urban canyon effects, intensifying multipath errors. In high precision surveying, particularly in Real-time Kinematics (RTK) and static GNSS surveys, multipath can significantly cause positional

inaccuracies ranging from a few centimeters to several meters (Khider et al., 2018). Given the growing reliance on GNSS technology for campus-related activities ranging from construction layout and mapping to research and navigation it becomes crucial to analyze how multipath affects positioning within the University of Benin. Such an analysis will help determine the extent of positional errors across different campus environments, identify multipath-prone areas, and develop strategies for minimizing their impact. While GNSS has revolutionized positioning and navigation, its effectiveness is challenged by multipath interference especially in environments like that of the University of Benin. By analyzing this effect in detail, this research contributes to the broader goal of enhancing positioning accuracy and reliability in real-world applications. This study investigates multipath effects on GNSS positioning accuracy within the University of Benin.

1.2 Statement of the Problem

Although GNSS has greatly improved the way surveyors and engineers determine precise positions, the issue of multipath error remains a serious challenge, especially in environments surrounded by reflective objects. Under open-sky conditions, GNSS signals mainly suffer from predictable errors such as atmospheric delays or satellite clock biases. In areas with buildings, trees, or vehicles like most parts of the University of Benin reflected signals can distort measurements and reduce the accuracy of the results.

Many existing GNSS processing systems use simple stochastic models that depend only on satellite elevation angles to estimate observation quality. These models assume that signals from satellites at similar elevations have similar accuracy. In reality, however, this is not true because signal quality also depends on factors such as the signal-to-noise ratio (SNR), azimuth angle, and

local surroundings. Ignoring these factors makes the computed variance-covariance matrix less representative of the actual data quality.

Furthermore, most multipath modeling studies have been carried out in developed countries using expensive commercial software and specialized equipment. There is little locally developed research using open-source tools like RTKLIB in Nigerian or African contexts. This creates a gap in understanding how multipath behaves in our unique environments and how best to model it.

There is therefore a need to develop a realistic, site-specific stochastic model that accurately represents the variation in GNSS observation noise under both open-sky and multipath conditions. Such a model will help improve positioning accuracy and provide a deeper understanding of how multipath errors behave spatially across different environments within the University of Benin.

1.3 Aim and Objectives of the Study

The aim of this study is to develop and apply a stochastic model for quantifying multipath errors in static GNSS observations using RTKLIB, with a case study focused on the University of Benin.

The objectives are to:

I. develop a stochastic model for pseudorange observations under open-sky conditions.
II. apply the developed stochastic model to multipath-prone GNSS observations for variance analysis.
III. quantify and characterize the spatial distribution of multipath errors in static GNSS observations.

1.4 Scope and Limitation of the Study

This research is limited to the analysis of static GNSS data collected within the University of Benin. It will focus mainly on pseudorange measurements obtained under both open-sky and multipath-prone conditions. The analysis will be performed using the open-source software RTKLIB, supported by other data analysis tools such as MATLAB or Python for statistical modeling, visualization, and mapping.

The study will not include dynamic (moving) GNSS applications, real-time correction techniques such as RTK or PPP, or data from all GNSS constellations beyond GPS and GLONASS. Atmospheric errors like ionospheric and tropospheric delays will be handled using standard broadcast models, as the focus is mainly on understanding the stochastic nature of multipath effects rather than correcting deterministic errors.

Some limitations may arise due to factors such as receiver sensitivity, limited observation time at each station, changing weather conditions, and the presence of obstacles that may affect signal strength. Despite these, every effort will be made to collect quality data and ensure that the results accurately reflect the true behavior of multipath errors in the study area.

1.5 Justification of the Study

Accurate and reliable positioning is fundamental to a wide range of academic, professional, and infrastructural activities. From engineering surveys and geospatial mapping to campus planning and research, the use of GNSS (Global Navigation Satellite System) technologies has become increasingly important within the University of Benin. However, the reliability of GNSS data is

often compromised by multipath interference, especially in areas surrounded by reflective surfaces such as buildings, trees, and metal structures.

Despite the widespread application of GNSS-based tools on campus, there exists a significant knowledge gap regarding how environmental conditions, especially multipath, affect positioning accuracy. Many students, researchers, and field technicians rely on GNSS devices without fully understanding the errors introduced by reflected signals. This oversight can lead to serious consequences such as data misinterpretation, flawed engineering designs, inaccurate spatial analyses, and general inefficiency in fieldwork. The findings from this study will contribute to the growing body of knowledge in GNSS error modeling and environmental analysis within the University of Benin. In summary, this study is justified by its practical relevance, academic contribution, and potential to improve GNSS-based positioning outcomes within the University of Benin and serve as a reference for other institutions experiencing similar challenge

CHAPTER TWO

LITERATURE REVIEW

2.0 History and Evolution of GNSS

The development of Global Navigation Satellite Systems (GNSS) began in the late 1950s, inspired by the launch of Sputnik I, when scientists realized that satellite signals could be used for positioning by analyzing the Doppler effect. This early concept led to the creation of the TRANSIT system in the 1960s, the first operational satellite navigation system, which provided limited but valuable positioning data primarily for military use. The major breakthrough came in the 1970s with the U.S. Department of Defense's development of the NAVSTAR Global Positioning System (GPS). GPS aimed to provide continuous, global, real-time positioning and timing information. The first GPS satellite was launched in 1978, and by 1995, the system reached full operational capability with a complete constellation of 24 satellites (Kaplan and Hegarty et al., 2017). Initially, civilian access was limited by Selective Availability, but this was discontinued in 2000, vastly improving civilian positioning accuracy. Following GPS, other nations developed their own satellite navigation systems to provide independent capabilities and improve coverage. Russia's GLONASS became operational in the 1990s and after some setbacks, was fully restored in the early 2010s. Misra and Enge (2011). The European Union developed Galileo, a civilian-controlled system designed to provide high-precision services and ensure strategic autonomy, with operational services beginning in 2016. China's BeiDou system evolved from regional coverage in the early 2000s to global coverage by 2020, completing the modern set of global constellations.

Recent decades have seen significant modernization of these systems, including the addition of new civilian signals, improved accuracy, resistance to interference, and integration of multiple GNSS constellations in single receivers. Newer GNSS signals are designed to be more robust against reflections and allow for better multipath detection and mitigation at the receiver level. (Bhatta et al., 2010). These advances have enabled more reliable positioning in challenging environments such as urban areas and university campuses. Augmentation systems further enhance accuracy and reliability, expanding GNSS applications across fields including surveying, agriculture, disaster management, and everyday mobile navigation. The evolution of GNSS has greatly impacted the field of surveying by transforming traditional methods into highly precise and efficient processes. Modern GNSS surveying combines satellite data with augmentation systems and advanced processing algorithms to mitigate errors like multipath and atmospheric delays, achieving centimeter-level accuracy essential for engineering projects, land development, and geospatial data collection. Leick, Rapoport, and Tatarnikov (2015) mdocumented the evolution of GNSS surveying from static techniques to Real-Time Kinematic (RTK) which provide centimeter-level precision. This ongoing evolution continues to enhance surveying efficiency, accuracy, and cost-effectiveness, making GNSS an indispensable tool in the profession and enabling precise spatial analysis in diverse environments.

2.1 Overview of Positioning Systems

Positioning systems are technologies and methods used to determine the geographic location of objects or people on or near the Earth's surface typically through coordinate systems (Hofmann-Wellenhof et al., 2008). These systems play a critical role in navigation, mapping, surveying, and many other applications. Positioning systems can be broadly categorized based on the technology

they use, their operating environments (outdoor or indoor), and the type of signals they rely on. One of the most widely known positioning systems is the Global Navigation Satellite System (GNSS), which includes constellations such as GPS (United States), GLONASS (Russia), Galileo (European Union), and BeiDou (China). GNSS relies on a network of satellites that continuously broadcast signals to receivers on the ground. By calculating the travel time of these signals, GNSS receivers can determine their precise location in three-dimensional space. GNSS is highly effective in open outdoor environments, providing global coverage with accuracy ranging from a few meters to centimeters when augmented with additional techniques. Bhatta et al., (2010) describes GNSS positioning as the process of using satellite signals to calculate the 3D coordinate of a point. Besides satellite-based systems, ground-based positioning techniques also exist. These include terrestrial radio navigation systems like LORAN (Long Range Navigation), which use fixed ground transmitters to provide location information. More recent developments in wireless positioning use signals from cellular networks, Wi-Fi access points, or Bluetooth beacons, enabling location estimation in urban and indoor environments where satellite signals are often weak or unavailable. Indoor positioning systems have become increasingly important with the rise of smart buildings and location-based services. Unlike GNSS, which struggles indoors due to signal attenuation and multipath effects caused by walls and other structures, indoor systems rely on alternative technologies such as Ultra-Wideband (UWB), inertial measurement units (IMUs), or magnetic field mapping to estimate position within buildings.

Hybrid positioning systems combine multiple technologies and signal sources to enhance accuracy, reliability, and availability. For example, combining GNSS with inertial navigation systems or using multiple satellite constellations simultaneously can mitigate common problems such as signal blockage, interference, and multipath effects. Recently, researchers have adopted

3D city models, ray-tracing algorithms, and AI-based prediction models to identify likely multipath zones in advance of surveying (Zhao et al., 2020). In summary, positioning systems encompass a wide array of technologies designed to meet diverse needs, ranging from global outdoor navigation to precise indoor localization. Understanding the strengths and limitations of each system is vital for addressing challenges such as multipath interference, particularly in complex environments like the University of Benin campus.

2.2 Ground based Positioning Techniques

Ground-based positioning techniques utilize terrestrial infrastructure and signals to determine the location of an object or person, serving as either an alternative or complement to satellite-based systems like GNSS. These techniques are particularly valuable in environments where satellite signals are weak, obstructed, or unavailable, such as indoors, urban canyons, or heavily forested areas. Even under controlled GNSS setups, residual position errors ranging from 1.3mm to 3.3mm in planimetric and 3.5mm to 6.7mm in height. Akhigbe, R.A, Oladosu, S.O., & Ehigiator-Irughe, R. (2023). One of the earliest ground-based navigation systems is LORAN (Long Range Navigation), developed during World War II. LORAN used low-frequency radio signals transmitted by fixed ground stations to enable navigation by measuring the difference in signal arrival times. Although largely replaced by GNSS, variations of LORAN, such as eLORAN, are still explored for backup navigation and positioning due to their robustness and resistance to jamming. In more recent times, positioning techniques leveraging cellular networks have become widespread. Mobile devices can estimate their position by analyzing signal strengths, time delays, or angle of arrival from multiple cellular base stations. This method, often called cellular

triangulation or multilateration, offers reasonable accuracy in urban and suburban areas where cellular coverage is dense.

Wi-Fi-based positioning systems utilize signals from wireless access points to provide location information, especially indoors. By mapping the geographic locations of Wi-Fi hotspots and measuring signal strengths, devices can approximate their position through fingerprinting or proximity techniques. This approach has become integral to indoor navigation applications in malls, airports, and large campuses.Other ground-based methods include the use of Bluetooth Low Energy (BLE) beacons, Ultra-Wideband (UWB) systems, and infrared or ultrasonic signals. These technologies offer varying degrees of accuracy and range, with UWB known for its high precision in indoor environments, often achieving centimeter-level accuracy. Such systems are particularly useful for asset tracking, robotics, and indoor way finding. Ground-based positioning techniques often complement GNSS by providing enhanced accuracy (millimeter level) and availability in challenging environments. (Leick et al. 2015). They also serve critical roles where GNSS signals are intentionally degraded or unavailable due to signal blockage, interference, or regulatory constraints. In summary, ground-based positioning techniques offer essential solutions to the limitations of satellite navigation, enabling reliable location determination in diverse settings. Their integration with satellite systems and advances in wireless communication technologies continue to expand the possibilities for precise and ubiquitous positioning.

2.3 Indoor vs Outdoor Positioning Systems

Positioning systems can be broadly categorized based on the environments in which they operate—outdoor and indoor. Each environment presents unique challenges and requirements that influence the choice of technology, system design, and performance capabilities. Outdoor positioning

systems predominantly rely on satellite-based technologies such as Global Navigation Satellite Systems (GNSS), which provide global coverage by transmitting signals from satellites orbiting the Earth. (Bhatta et al., 2010). GNSS receivers calculate their position by measuring the time delay from multiple satellites, offering reliable and accurate positioning in open outdoor environments. These systems are widely used for navigation, surveying, mapping, and many location-based services where clear line-of-sight to satellites is available. However, outdoor positioning can still be affected by factors such as atmospheric conditions, signal multipath, and obstructions like tall buildings or dense foliage.

In contrast, indoor positioning systems face more complex challenges due to the signal attenuation, reflection, and scattering caused by walls, furniture, and other structural elements. Satellite signals generally cannot penetrate buildings effectively, rendering GNSS unreliable indoors. To address this, indoor positioning relies on alternative technologies including Wi-Fi, Bluetooth Low Energy (BLE) beacons, Ultra-Wideband (UWB), inertial sensors, magnetic field mapping, and infrared or ultrasonic signals. These technologies enable the tracking and localization of devices and assets within buildings, supporting applications like indoor navigation, asset management, and emergency response. While indoor systems often prioritize short-range communication and high accuracy within confined spaces, outdoor systems emphasize broad coverage and robustness over larger areas. Additionally, indoor systems frequently integrate multiple technologies and sensor data to improve accuracy and reliability, compensating for the complexities of indoor signal environments. Hybrid systems that combine outdoor GNSS with indoor positioning technologies are increasingly common due to their ability to maintain positioning performance in GNSS-challenged areas providing seamless location tracking as users move between outdoor and indoor environments. (Jin et al.,2022). Understanding the differences between indoor and outdoor

positioning systems is essential for selecting appropriate solutions and mitigating issues such as multipath interference and signal loss by triangulating signals from non-GNSS sources. (Zafari et al. 2019). For environments like the University of Benin campus, where users may frequently transition between outdoor open spaces and indoor facilities, leveraging both types of positioning systems is crucial for comprehensive location-based services and precise surveying applications.

2.3.1 Previous Research on Positioning in Nigerian Universities

In the Nigerian context, studies focused on GNSS positioning within university environments are still relatively limited, though a few notable contributions exist. Research efforts have explored the use of GPS and total station technology for cadastral mapping, infrastructure planning, and geodetic surveys within Nigerian campuses such as the University of Lagos (Alabi et al., 2024), Obafemi Awolowo University, and Ahmadu Bello University. (Isioye et al., 2019). These studies often report challenges related to satellite visibility, poor GNSS signal reception, and errors caused by multipath in built-up areas. For example, an assessment of GPS accuracy within Obafemi Awolowo University found that signal blockage and multipath from building walls and trees significantly reduced positional accuracy, with standard deviation values exceeding expected thresholds for precise survey applications. While these studies offer insights into the performance of GNSS in Nigerian academic settings, there remains a noticeable gap in systematic analysis focused specifically on multipath propagation patterns and their quantifiable impact on positioning. The University of Benin, with its unique combination of dense faculties, large vegetation zones, and varying infrastructure, presents an important case for further investigation.

2.4 Global Navigation Satellite Systems (GNSS)

Global Navigation Satellite Systems (GNSS) refer to satellite constellations that provide autonomous geo-spatial positioning with global coverage. These systems allow a GNSS receiver to determine its precise location (latitude, longitude, and altitude) anywhere on or near the Earth by receiving signals from multiple satellites and calculating the travel time of those signals. GNSS technology has become fundamental in numerous applications including navigation, surveying, mapping, timing, and scientific research. GNSS has become a useful tool for Earth science, contributing to meteorology, geology, oceanography, and climate research through innovative remote sensing techniques (Jin et al., 2022). The most widely known and extensively used GNSS is the United States' Global Positioning System (GPS), which was developed initially for military purposes but is now freely accessible for civilian use worldwide. GPS operates through a constellation of at least 24 satellites orbiting approximately 20,200 kilometers above the Earth, continuously transmitting signals on multiple frequencies. Multi-constellation PPP not only improves accuracy but also enhances resilience to multipath-related signal degradation especially at low satellite elevation (Li et al. 2015). By measuring the time delay between the transmission and reception of signals from at least four satellites, a GPS receiver can accurately calculate its three-dimensional position and precise time. In addition to GPS, other GNSS constellations have been developed to provide global or regional coverage and to improve system reliability and accuracy. Russia's GLONASS is a fully operational global system similar to GPS, offering an alternative set of satellites that enhances positioning availability, especially in high-latitude regions. The European Union's Galileo system is designed to provide highly accurate and reliable positioning services with improved signal integrity and timing, supporting both civilian and commercial applications (European Commission, 2024). China's BeiDou system started as a

regional network and has expanded into a global constellation, contributing further to the diversity of available satellite signals. BeiDou provides strong satellite visibility in the Asia-Pacific region, often outperforming other constellations in terms of satellite count in this region (Gao et al., 2023)

Modern GNSS receivers often utilize signals from multiple constellations simultaneously, a practice known as multi-constellation GNSS. This approach improves positioning accuracy, availability, and robustness, especially in challenging environments such as urban canyons, dense foliage, or university campuses where signal obstruction and multipath propagation are common. Despite their advantages, GNSS signals are susceptible to various errors caused by atmospheric conditions, satellite geometry, clock inaccuracies, and environmental factors such as multipath effects. Multipath occurs when satellite signals reflect off surfaces like buildings or the ground before reaching the receiver, causing delays and interference that degrade positioning accuracy. Understanding these limitations is crucial in applying GNSS technology effectively in precision-dependent fields such as surveying and engineering. Overall, GNSS remains the backbone of modern positioning systems, providing essential location and timing information for a wide range of applications globally.

2.4.1 Case Studies on GNSS Accuracy in Challenging Terrains

Beyond academic institutions, a number of case studies have investigated GNSS accuracy in environments with similar complexities, such as urban centers, forested zones, and mountainous terrains. These environments exhibit high levels of multipath and signal attenuation, similar to campus settings. A study conducted in Tokyo’s urban core revealed how GNSS receivers often locked onto reflected signals, mistaking them for direct signals, resulting in position errors of up to 20 meters.(Tokyo, Japan, 2024). Another study in forested regions of South America showed

that canopy reflections led to low signal-to-noise ratios and increased noise in carrier-phase measurements, degrading the quality of RTK solutions (RTK performed in forest 2024). Some researchers have employed 3D ray-tracing and simulation techniques to model signal behavior in complex terrains, improving understanding of how multipath develops in real-world environments. (Pant et al., 2022). These models have been effective in predicting error hotspots and guiding optimal antenna placement to reduce interference. The application of such techniques to university environments, such as the one in this study, holds potential for improving GNSS-based survey practices. They also underscore the relevance of combining empirical fieldwork with analytical modeling to fully characterize and mitigate multipath effects.

2.5 Multipath Propagation

Multipath propagation is a significant phenomenon that affects the accuracy and reliability of positioning systems, particularly those based on radio signals such as GNSS, it is systematic and difficult to eliminate (Hofmann-Wellenhof et al. 2008). It occurs when transmitted signals reach the receiver by multiple paths instead of a single direct path, causing interference that can distort the true signal and lead to positioning errors. Multipath propagation refers to the reception of a radio signal by a receiver through several different paths, caused by reflection, diffraction, and scattering of the signal waves from surfaces or obstacles before reaching the receiver antenna. Instead of arriving via a direct line-of-sight, the signal arrives in multiple copies, each having traveled a different route and thus experiencing different delays and phase shifts. Common causes of multipath include natural and man-made structures such as buildings, trees, vehicles, and terrain features. In urban and campus environments, the abundance of reflective surfaces like glass windows, metal structures, and concrete walls increases the likelihood of multipath. Multipath is

one of the most challenging errors to mitigate in GNSS positioning. (El-Rabbany et al., 2022). Additionally, moving objects such as vehicles or people can dynamically change the signal paths, creating time-varying multipath effects.

2.5.1 Stochastic Representation of Pseudorange Observations under Open-Sky Conditions

Several studies have focused on developing observation variance models for pseudorange and carrier-phase data under more benign (open-sky) conditions, which then form a baseline for comparison or model-development under multipath-rich environments. For example, Medina et al. (2018) produced probabilistic pseudorange error models using inverse-Gamma priors and large dynamic datasets and characterized multipath contributions under signal-degraded environments. Their work demonstrated that the variance-covariance matrix of observables must explicitly include a multipath term, in addition to classical error sources (e.g., satellite clock, troposphere). Similarly, Lau (2021) reviewed GNSS multipath errors and mitigation techniques, noting that pseudorange multipath can reach magnitudes of a few meters and is seldom explicitly modelled in standard data processing. These underpin the necessity of constructing stochastic models that reflect realistic (non-homoscedastic) observational conditions before applying them in multipath-rich settings.

2.5.2 Stochastic Representation of Multipath-Prone GNSS Data

In transitions from open-sky to multipath-rich settings, the adaptation of stochastic models and the analysis of variance behaviour become crucial. For instance, Uaratanawong et al. (2020) explored pseudorange multipath mitigation through satellite-selection method such as elevation and SNR masks, in single-point positioning (SPP) tests in multipath environments, concluding that an SNR

mask of ~36 dB-Hz improved horizontal accuracy by about 46.8%.. Another study by Zou et al. (2021) applied fusion modelling methods for multi-GNSS (GPS, BDS, Galileo) and pioneered a space-domain multipath error mitigation approach (MHGM) that uses multi-day data to improve modelling of multipath variation. Their results underscore that long-term multi-day modelling substantially enhances mitigation of multipath in multi-GNSS scenarios. Such work demonstrates how stochastic modelling and variance analysis must adapt when the observational conditions shift from open-sky to multipath-prone. The stochastic representation of multipath-prone GNSS data focuses on modeling how random signal reflections influence the statistical behavior of pseudorange and carrier-phase observations. Unlike deterministic error sources such as satellite clock bias or ephemeris error, multipath is inherently random, environment-specific, and time-varying. Consequently, its effects cannot be completely eliminated by functional modeling alone; instead, they must be statistically represented within the stochastic model that governs the weighting and variance covariance structure of GNSS observations. In conventional GNSS processing, a simple stochastic model assumes that all pseudorange observations possess identical variance and are uncorrelated. This assumption, though convenient, is unrealistic in environments affected by multipath. In multipath-prone conditions, the variance of each observation depends on several factors such as satellite elevation angle, signal-to-noise ratio (SNR), antenna design, reflecting surface geometry, and temporal correlation of reflections. Hence, the stochastic model must be flexible enough to accommodate these dependencies.

2.5.3 Characteristics of Multipath in Urban and Campus Environments

A core objective of the present research is the spatial characterization of multipath errors. In this vein, Nour et al. (2019) investigated how antenna height influences multipath in a real-time

kinematic (RTK) GNSS setup and found strong inverse relationships between antenna height and pseudorange/phrase multipath error magnitude highlighting how local geometry modifies signal reflections. Moreover, other research (Khanafseh et al., 2018) provided empirical over-bounding statistics for pseudorange and carrier-phase multipath under open-sky and near-reflector conditions, and determined time-correlation constants for multipath error processes. Such spatial and temporal characterizations help in understanding how multipath errors vary across azimuth/elevation, environment type (urban canyon vs open-sky), and over time—information necessary for mapping error distribution and designing mitigation schemes. Urban and campus environments present particularly challenging conditions for positioning systems due to the prevalence of multipath propagation. In urban areas, tall buildings, narrow streets, and dense infrastructure create “urban canyons” where GNSS signals are frequently blocked, reflected, or diffracted. This can cause significant positioning errors, signal fading, and loss of satellite visibility. (Misra and Enge 2011). Similarly, university campuses, like the University of Benin, typically contain a mixture of open spaces and complex built environments with classrooms, administrative buildings, trees, and other structures. These features create a heterogeneous propagation environment where multipath effects are highly site-specific and can vary throughout the day as satellite geometry and environmental conditions change. Multipath in these settings leads to distortions such as signal delay and phase shifts, which degrade the accuracy of pseudorange and carrier phase measurements fundamental to GNSS positioning. Understanding the spatial and temporal behavior of multipath is essential for developing effective mitigation techniques and ensuring reliable positioning performance in such environments.

2.5.4 Effects of Multipath on Positioning Accuracy

Multipath propagation significantly affects the accuracy and reliability of positioning systems, especially those relying on GNSS signals. The multiple signal paths resulting from reflections, diffractions, and scattering introduce errors in the measured signal parameters, leading to degraded positioning performance.

2.5.5 Detection and Mitigation of Multipath Effects

To bring these strands together stochastic modelling, variance analysis, spatial characterization the recent study by Park, Yoon, and Lee (2024) is particularly relevant. They propose using pseudorange range acceleration (RA) the second derivative of pseudorange time series via three consecutive epochs as a dynamic weight in least squares estimation. Their rationale is that multipath-affected signals show significant fluctuations in RA, whereas clean line-of-sight signals present near-zero RA. Their field results demonstrate positioning accuracy improvements of up to 75% horizontally and 79% vertically when using RA weighting alone, and over 80% improvement when combining RA with an SNR threshold in deep urban environments. This demonstrates a concrete method of applying stochastic weighting to multipath-prone observations and offers insight into a spatially sensitive metric (RA fluctuations tied to local multipath) relevant to characterization the spatial distribution of multipath errors. Multipath propagation poses a persistent challenge in achieving accurate positioning, particularly in complex environments such as urban areas and university campuses. Effective detection and mitigation of multipath effects are essential to enhance the performance of GNSS and other radio-based positioning systems. Various techniques have been developed, ranging from hardware improvements to advanced signal processing methods.

2.5.6 Receiver-Based Techniques

Receiver-based techniques focus on the capabilities within GNSS receivers to detect and minimize the influence of multipath signals. Modern receivers employ advanced correlator designs, such as narrow correlators and multipath estimating delay lock loops (MEDLL), to distinguish the direct signal from delayed multipath replicas. These methods improve the receiver's ability to track the true line-of-sight signal by reducing the correlation peak's spread caused by multipath. Additionally, receivers can use signal quality indicators, such as signal-to-noise ratio (SNR) and multipath error estimates, to identify and reject corrupted measurements (El-Rabbany et al., 2002). Some receivers integrate multi-frequency and multi-constellation capabilities, which allow them to cross-check measurements across different signals, enhancing the detection of anomalous multipath-affected data.

2.5.7 Antenna Design and Placement

Antenna design plays a crucial role in mitigating multipath effects by physically minimizing the reception of reflected signals. Specialized GNSS antennas incorporate features such as choke rings, ground planes, and hemispherical radomes to suppress signals arriving from low elevation angles, where reflections are more likely to occur. These antennas effectively reduce multipath by filtering out signals reflected from the ground and nearby surfaces, but when improperly placed can introduce significant biases especially in code-based measurements, due to its vulnerability to reflected signals. (Hofmann-Wellenhof et al., 2008). Proper antenna placement is equally important. Positioning antennas away from reflective surfaces, such as walls, metal structures, and large bodies of water, helps minimize the incidence of multipath. On campuses or urban sites, elevating the antenna and selecting open, unobstructed locations can significantly improve signal

quality. Using tripod mounts or masts to isolate antennas from nearby reflective objects is a common practical mitigation approach.

2.5.8 Multipath Analysis in Academic Environments

Academic institutions often present complex signal environments due to the diversity in building structures, open spaces, vegetation, and human movement. Several studies have investigated the influence of multipath propagation in such settings, emphasizing the variability and site-specific nature of signal degradation. For instance, research conducted in European and Asian universities has shown that signal reflections from glass windows, concrete walls, and metallic fixtures within campuses can introduce significant GNSS errors, especially in static and kinematic surveys. Angskog et al., (Sweden 2015). In many cases, errors due to multipath were found to range between 1-10 meters in pseudorange measurements, and even greater inaccuracies in carrier-phase solutions during real-time navigation tasks. (Sathyamoorthy et al., 2015). Moreover, studies have evaluated the effectiveness of GNSS augmentation systems such as Real-Time Kinematic (RTK) and Differential GPS (DGPS) in academic environments. Results indicated that although these methods improved positioning accuracy, their performance was still hindered by persistent multipath, particularly in areas surrounded by tall buildings and dense infrastructure. Such findings highlight the necessity of site-specific multipath analysis in academic environments like the University of Benin.

2.6 Signal Delay and Pseudorange Errors

One of the primary effects of multipath is signal delay, where reflected signals travel longer paths before reaching the receiver compared to the direct line-of-sight signal. This additional travel time

causes the receiver to overestimate the distance to the satellite, known as pseudorange error. Since positioning calculations depend heavily on accurate distance measurements from multiple satellites, these errors propagate into the final position solution, resulting in spatial inaccuracies that can range from a few meters to tens of meters in severe cases. Pseudorange errors caused by multipath are particularly problematic in environments with many reflective surfaces, such as urban or campus settings. (Misra and Enge 2011). These errors vary dynamically as the satellite geometry and environmental conditions change, making them challenging to predict and compensate.

2.6.1 Phase Shifts and Interference

Multipath signals not only introduce delay but also cause phase shifts due to differences in path length and signal reflection characteristics. When the reflected signals combine with the direct signal at the receiver antenna, they can interfere constructively or destructively, altering the amplitude and phase of the received signal. This interference can lead to fluctuations in the carrier phase measurements, which are crucial for high-precision positioning techniques. Phase errors degrade the quality of the signal tracking and can cause cycle slips or loss of lock, reducing the reliability of the positioning system. The phase distortion caused by multipath complicates the extraction of accurate measurements, particularly in high-precision applications like geodetic surveying requiring robust correction models.(Leick et al 2015).

2.6.2 Impact on Real-Time Kinematic (RTK) and Differential GPS (DGPS)

Advanced GNSS techniques such as Real-Time Kinematic (RTK) and Differential GPS (DGPS) rely on precise measurements of pseudorange and carrier phase to achieve centimeter to decimeter

level accuracy. Multipath significantly impacts these systems by introducing errors that cannot be fully eliminated through differential corrections.(Hofmann-Wellenhof et al., 2008) In DGPS, reference stations transmit correction signals to rovers, which helps reduce common satellite and atmospheric errors. Nevertheless, multipath errors, being highly local and environment-specific, are not always correlated between the reference station and rover, limiting the effectiveness of DGPS corrections. (El-Rabbany et al., 2002). RTK positioning, which depends on carrier phase measurements, is even more sensitive to multipath. (Jin et al., 2022). Phase distortions caused by multipath can result in incorrect ambiguity resolution, which is the process of determining the exact number of whole carrier wavelengths between the satellite and receiver. This leads to degraded positioning accuracy or even complete failure of the RTK solution, especially in multipath-rich environments like urban areas or dense campuses. Understanding the effects of multipath on these high-precision positioning methods is crucial for developing mitigation strategies and improving system reliability in environments prone to signal reflections.

2.6.3 Signal Processing and Filtering Algorithms

Advanced signal processing techniques help isolate the direct line-of-sight signal from delayed (reflected) signals, thereby improving position accuracy, especially in multipath-dense environments like cities or construction zones. (Misra and Enge et al., 2011). Kalman filtering and other Bayesian approaches are commonly used to smooth position estimates by combining current measurements with predictions based on motion models, effectively reducing noise and multipath distortions. Some algorithms exploit the temporal and spatial correlation of multipath signals to differentiate them from direct signals. Moreover, integration of GNSS data with inertial measurement units (IMUs) or other sensor inputs through sensor fusion methods provides robust

positioning solutions that are less susceptible to multipath errors. These approaches are particularly beneficial in dynamic environments like university campuses, where multipath conditions vary frequently.

2.7 Summary of Literature Gaps

The review of existing literature on positioning systems and multipath propagation reveals considerable advancements in understanding and mitigating positioning errors caused by signal reflections and interference. However, several key gaps still persist, particularly in relation to localized, environment-specific studies such as university campuses in Sub-Saharan Africa, including Nigeria. These gaps justify the need for the present study and serve as a foundation for its objectives and methodology.

I. Limited Contextual Research in Nigerian Academic Environments

   while there is an abundance of global research on GNSS performance in urban, forested, and mountainous terrains, the specific context of Nigerian universities has been sparsely explored. Most available studies in Nigeria focus on broad applications of GPS for cadastral surveys, land use planning, or navigation, without delving deeply into the environmental factors influencing GNSS errors especially multipath. There is a lack of rigorous, location-specific analysis of multipath effects on positioning accuracy in educational institutions like the University of Benin, despite the obvious presence of signal-distorting features such as tall faculty buildings, metal structures, and vegetation.

II. Inadequate Focus on Multipath as a Primary Source of Error

   Several Nigerian-based GNSS studies acknowledge error sources in general terms such as atmospheric delay, signal blockage, and satellite geometry but tend to treat multipath

interference as a secondary concern or fail to isolate it altogether. This results in a shallow understanding of how multipath uniquely affects both static and dynamic positioning solutions in structurally complex environments like university campuses. There is a clear need for studies that isolate and analyze multipath errors, both temporally and spatially, to better understand their variability and impact on precise positioning.

III. Insufficient Empirical Validation Using Local Data

Most multipath-related models and error correction techniques reviewed in literature are based on simulations or fieldwork in developed countries with different infrastructure and signal environments. There is minimal empirical validation using real-world data collected within Nigerian terrain, topography, and building typologies. As such, the applicability of foreign-based findings or solutions remains questionable in the Nigerian context. Localized empirical studies such as the one being undertaken in the University of Benin are crucial to validating or challenging these broader models in order to develop contextually appropriate strategies for mitigation.

IV. Lack of Campus-Based Multipath Characterization

Academic institutions, especially those with large campuses like the University of Benin (Ugbowo), contain a mix of indoor and outdoor environments, heavy foot and vehicle traffic, varying building heights, and diverse vegetation. These factors contribute to unique multipath scenarios. Despite this, existing research largely overlooks campuses as standalone case studies for positioning analysis. There is a gap in systematic research that maps signal behavior across different zones within a campus, assesses variations in signal quality and positioning error, and links these directly to structural or environmental features.

V. Absence of Combined Technical and Practical Evaluations

many studies focus either on the technical modeling of multipath or on its practical implications for positioning accuracy, but rarely both. There is a shortage of integrative studies that combine signal behavior analysis with surveying outcomes such as changes in coordinate measurements, baseline shifts, or survey repeatability errors due to multipath. Bridging this gap is essential for developing actionable insights that surveyors, planners, and GIS professionals can implement directly in campus environments.

VI. Underutilization of Modern GNSS Tools and Analytical Software

several previous research efforts, particularly in local academic settings, fail to utilize advanced GNSS tools and software capable of detailed multipath detection and mitigation. Tools such as GNSS-SDR, RTKLIB, or advanced post-processing software remain underexplored, leaving a technological gap in the methodology of existing works. Integrating these tools with local field measurements could provide more accurate analysis and richer datasets for decision-making.

VII. Minimal Recommendations for Environment-Specific Mitigation Techniques

Even in the few cases where multipath is acknowledged as a problem, mitigation strategies are often general and not tailored to the surveyed environment. Techniques such as optimal antenna placement, selection of appropriate survey windows based on satellite geometry, and use of hybrid positioning methods (e.g., GNSS + IMU) are seldom customized to reflect the unique structural and spatial layout of Nigerian campuses.

CHAPTER THREE

METHODOLOGY

3.1 Description of Study Area

This study primarily focused on the Ugbowo Campus of the University of Benin (UNIBEN), due to its larger area, more diverse infrastructure, and higher GNSS signal usage by engineering and geospatial programs. The University of Benin located in Benin City, the capital of Edo State, in Nigeria's South-South geopolitical zone. Originally established in 1970 as the Institute of Technology, the University was granted full university status by the National Universities Commission (NUC) in 1971 and renamed the University of Benin in 1972. The campus is geographically positioned between latitude 6°23′30″ N and 6°24′30″ N, and longitude 5°36′30″ E and 5°38′00″ E, with a central coordinate approximately at 6°23′50″ N, 5°37′23″ E. Ugbowo Campus straddles Ovia North-East Local Government Area and Egor Local Government Area, and it lies adjacent to the Benin-Lagos Expressway. The terrain of the University of Benin is generally undulating**,** with gentle slopes and low-lying areas. This location was selected due to its diverse mix of built-up infrastructure, vegetation, and open spaces, making it a suitable environment for studying the impacts of multipath propagation on GNSS positioning accuracy. The approach taken in this study is structured to ensure systematic data acquisition, processing, and analysis aimed at identifying and evaluating the extent to which multipath propagation impacts the accuracy of Global Navigation Satellite System (GNSS) positioning on campus including a detailed description of the study area, data collection techniques, equipment used, and analytical tools employed in quantifying multipath errors. This chapter also highlights the strategies that was used to validate the accuracy of results obtained and discusses any limitations encountered during

the research process. The selected methods was consistent with best practices in positioning and geospatial analysis, tailored specifically to the environmental and infrastructural characteristics of the University of Benin. By detailing each phase of the methodology, this chapter provides a clear roadmap for reproducing or extending the study, ensuring the reliability and transparency of the research process.

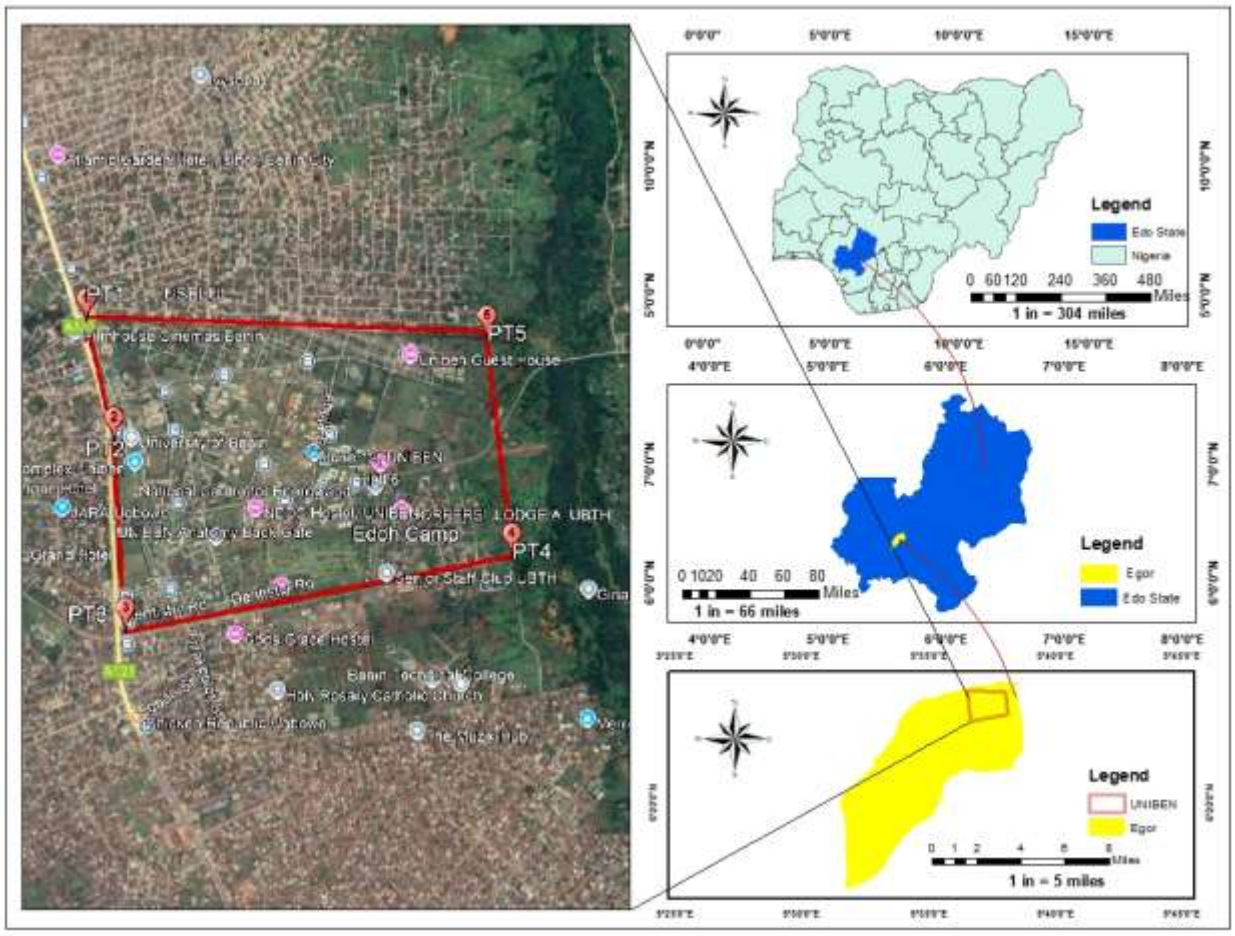

Fig 3.1: Study Area Map of University of Benin and Its Environment

3.2 Data Source

The data used in this study were obtained from static Global Navigation Satellite System (GNSS) observations collected using high-precision Tersus GNSS receivers. Two distinct datasets were acquired to represent contrasting signal environments: an open-sky site characterized by minimal obstructions and a multipath-prone site surrounded by reflective surfaces such as buildings and metallic structures. These contrasting setups provided the necessary conditions to analyze and quantify the influence of multipath on pseudorange measurements under real-world static conditions.

The observation data were recorded in Receiver Independent Exchange (RINEX) format, containing pseudorange, carrier phase, Doppler, and signal strength information for all tracked satellites. However, for the purpose of this study, only the pseudorange observations on the primary L1 frequency were extracted and analyzed. The open-sky dataset served as a reference for ideal signal conditions, while the multipath dataset captured measurement variations induced by reflected signals.

Each observation session lasted approximately one hour, ensuring sufficient temporal coverage for both environments to include a range of satellite geometries and elevation angles. The data were processed using RTKLIB, an open-source GNSS processing software, which generated residual statistics for each satellite and epoch. The resulting RTKLIB .stats file provided key parameters such as satellite elevation angle, carrier-to-noise ratio (C/N_0), and pseudorange residuals, variables essential for stochastic modeling.

Subsequently, the residuals and associated metadata were extracted from RTKLIB output files using a custom Python-based parser. This script systematically read and filtered the observation data to retain only valid measurements above defined signal strength and elevation thresholds. The filtered dataset formed the empirical basis for all subsequent analyses, including the development of the stochastic model and the quantification of multipath error.

In summary, the datasets used in this study originated from controlled static GNSS observations conducted under two environmental conditions and processed through an open-source analytical pipeline. This approach ensured that the derived stochastic parameters and multipath variance estimates were grounded in real observational data, accurately reflecting the statistical behavior of pseudorange errors in both ideal and multipath-affected settings.

3.3 GNSS Survey Planning

Strategic planning of the GNSS survey play a crucial role in this investigation, as it helps guarantee that satellite signals recorded during timeframes offering strong satellite presence and advantageous geometric arrangements. Survey planning is vital in reducing the impact of poor satellite geometry and ensuring reliable positioning. (Hofmann-Wellenhof et al., 2008). This step is vital, especially due to the study's emphasis on evaluating different satellite systems and the precision of derived positions. Before the commencement of field observations, the Trimble GNSS Online Planning Tool was employed to forecast satellite visibility and estimate Dilution of Precision (DOP) values specific to the Ugbowo Campus region (approximately 6°23′50″ N, 5°37′23″ E). This platform enabled the simulation of satellite trajectories for various global navigation systems such as GPS, GLONASS, Galileo, QZSS, and BeiDou, across a designated timeframe. To minimize the impact of low-angle signal degradation caused by the atmosphere and

multipath effects, an elevation mask of 15° was applied in filtering out satellites too close to the horizon.

The planning process spanned a full 24-hour cycle and includes evaluation of the following aspects:

I. Forecasted values for Position, Horizontal, and Vertical Dilution of Precision (PDOP, HDOP, VDOP)
II. Projected satellite paths shown in sky plots for all navigation constellations
III. Expected count of available satellites from each system
IV. Azimuth-elevation diagrams showing how satellites are distributed spatially above the horizon

This data-driven assessment supported the scheduling of GNSS observations during optimal time windows characterized by a minimum of 12 visible satellites and PDOP values ideally no higher than 2.0. These conditions was favorable for acquiring high-precision static positioning data. The visual outputs such as DOP graphs and sky view diagrams was documented and was used to substantiate the choice of observation times. They also served as interpretive tools when discussing how the arrangement of satellites affects positioning accuracy. Incorporating the Trimble planning interface into the data collection strategy ensured a standardized, reliable approach, preventing suboptimal satellite geometries and improving the quality of the gathered GNSS measurements. A consistent elevation cut-off threshold of 15° was maintained, following best practices, to exclude low-angle signals that are more likely to be degraded by atmospheric noise or reflect off nearby surfaces. (Leick et al., 2015).

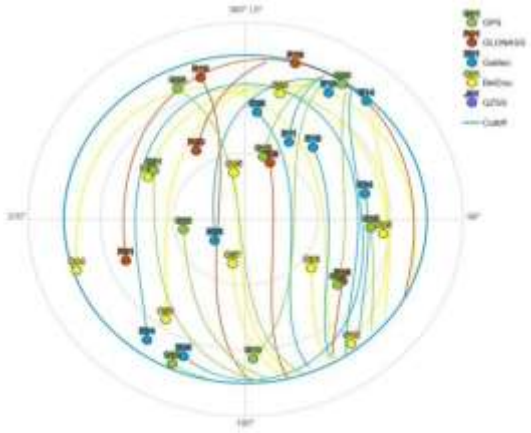

Fig. 3.2: Predicted Skyplot for Multi-GNSS Visibility over Ugbowo Campus (Elevation Mask: 15°)

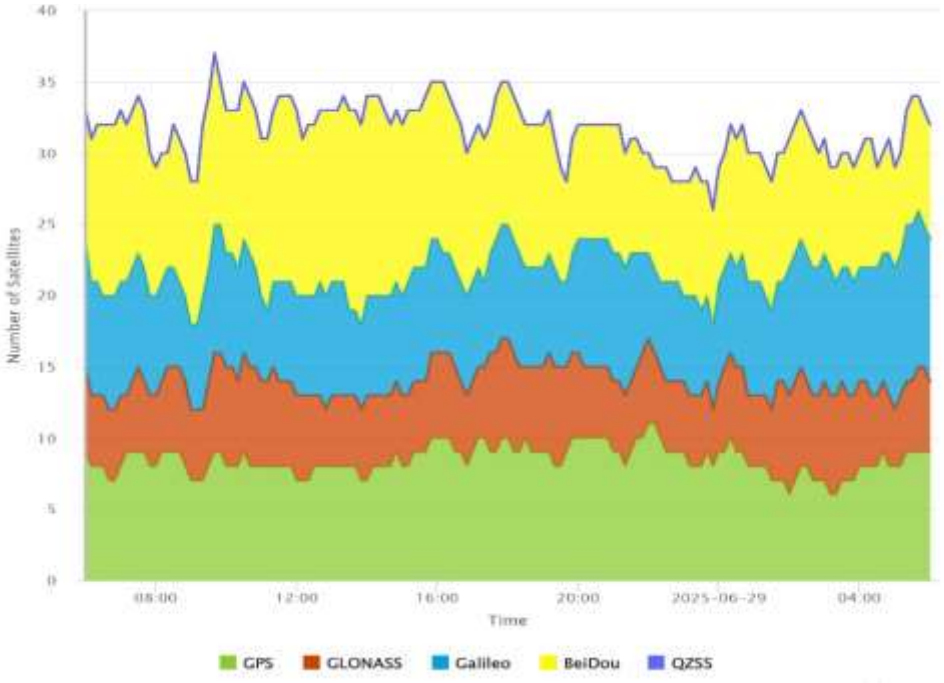

Fig. 3.3: Predicted Satellites Counts from Trimble GNSS Online Planning Tool

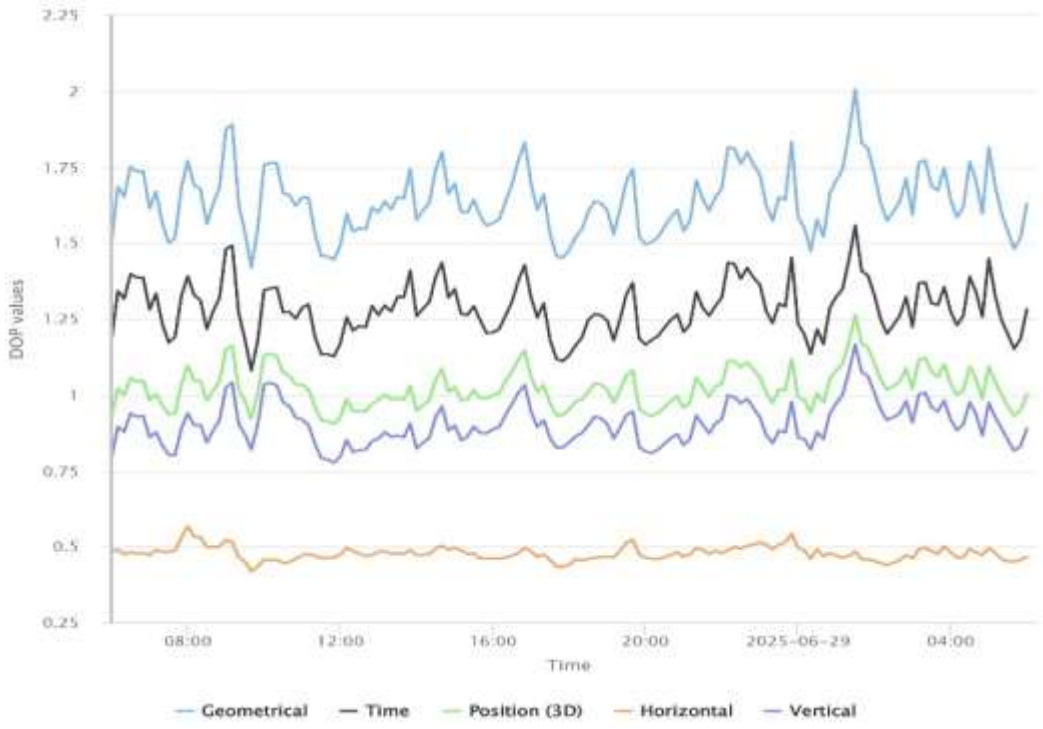

Fig. 3.4: DOPs Variation over 24 Hours from Trimble GNSS Online Planning Tool

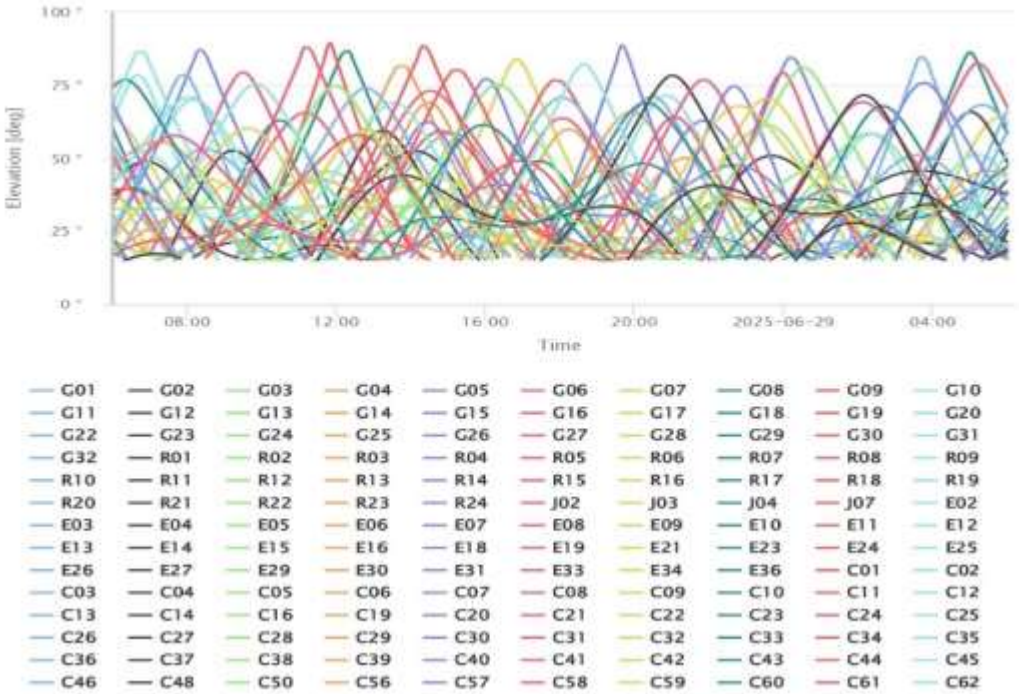

Fig. 3.5: Predicted Elevation of Satellites from Trimble GNSS Online Planning Tool

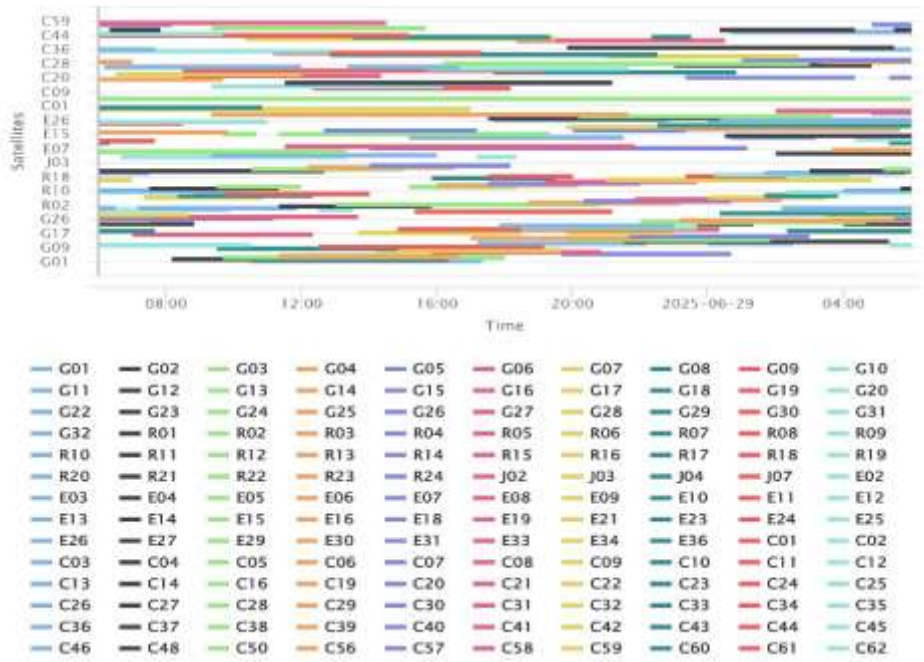

Fig. 3.6: Predicted Satellites Visibility from Trimble GNSS Online Planning Tool

3.4 DATA COLLECTION

At every control point, a Tersus David30 GNSS receiver was installed on a tribrach and firmly positioned on a tripod to maintain precise vertical alignment and centering above the designated survey mark. This configuration ensured a stable and reliable base for extended static data collection. The GNSS unit functioned in multi-frequency mode, capturing raw observation data that includes both pseudorange and carrier-phase measurements.

Fig. 3.7: Tersus David30 GNSS Equipment Setup at open-sky and multipath environment

The vertical distance from the survey marker to the Antenna Reference Point (ARP) of the Tersus David30 GNSS receiver was carefully measured using a tape, ensuring readings were taken as accurately as possible typically to the nearest meter. This receiver was mounted on a tribrach and positioned securely on a tripod. The recorded antenna height was later applied during post-processing to maintain vertical precision in the final coordinate solutions. At each control location, static GNSS observations was carried out continuously for one hour. Datas were collected at 5-second intervals, so as to allow for detailed satellite tracking and improved positioning resolution. This observation duration is strategically chosen to ensure sufficient satellite coverage, minimize short-term signal variations, and facilitate the evaluation of positioning accuracy across multiple satellite constellation scenarios. To enhance data quality and minimize the effects of unfavorable satellite configurations, pre-survey planning was performed using the Trimble GNSS Online Planning Tool. By entering the approximate coordinates of the study site (6°23′50″ N, 5°37′23″ E), the tool provided visual plots of satellite visibility, estimated satellite counts, and time-varying

PDOP (Position Dilution of Precision) values. Based on this information, observation sessions were scheduled during periods with optimal satellite geometry characterized by low PDOP and high satellite availability to maximize positional reliability, accuracy and multipath effect.

Fig. 3.8: GNSS Static Data Collection

Differential correction data was sourced from the GeoSys Continuously Operating Reference Station (CORS) to aid in enhancing the accuracy of post-processed GNSS results. This correction data helped mitigate errors related to satellite orbits and clock timing, thereby improving the reliability of the static positioning outcomes. For each observation session, detailed field records were maintained. These included documentation of atmospheric conditions like temperature and humidity, precise observation start and end times, as well as environmental factors such as sky visibility, physical obstructions, and potential sources of multipath interference. Where applicable, photographs were also captured to offer visual context of the surrounding signal environment. The

combination of raw GNSS observations and the CORS-derived correction inputs served as the foundational data for post-processing and evaluating coordinate precision.

3.5 Data Processing and Analysis

Post-processing forms a critical stage in this research, as it transforms the raw GNSS data collected from the field into precise positional information suitable for stochastic and statistical analysis. The central aim of this stage was to extract meaningful information on the behavior of pseudorange residuals and to quantify the extent of multipath error under varying observation conditions.

The raw observations recorded by the Tersus David30 receiver were initially stored in a proprietary format. These files were later converted into RINEX (Receiver Independent Exchange Format) using the Tersus data conversion tool. This conversion step was essential, as it standardized the data structure, allowing subsequent analysis and processing in RTKLIB, an open-source GNSS processing software that supports multi-constellation and multi-frequency observations. Each dataset was carefully trimmed to match the exact start and end times of observation at the control stations to ensure temporal consistency between rover and reference data.

The converted RINEX files were then processed in static differential mode using correction data obtained from the GeoSys Continuously Operating Reference Station (CORS). The CORS served as a fixed base, providing high-precision reference coordinates that enabled the mitigation of satellite orbit errors, clock biases, and atmospheric delays. This differential processing significantly enhanced the positional accuracy of the rover observations.

Following the coordinate computation, the pseudorange residuals, satellite elevation angles, and carrier-to-noise ratio (C/N_0) values were extracted directly from the RTKLIB statistical output file.

These residuals represent the difference between the observed and modeled pseudorange measurements and inherently contain the effects of unmodeled errors, including multipath. To ensure the integrity of the data used in subsequent analyses, the extracted values were subjected to a quality control procedure. Observations with incomplete epochs, loss of signal lock, or extremely low C/N_0 values were excluded. Additionally, elevation-based filtering was applied to eliminate satellites positioned too close to the horizon, as these are more susceptible to atmospheric interference and signal reflections.

The cleaned dataset was then prepared for stochastic modeling, which served as the foundation for quantifying multipath behavior. The statistical relationship between the variance of pseudorange residuals and satellite-dependent factors, specifically elevation angle and signal strength (C/N_0), was established through regression modeling. This analysis aimed to characterize how measurement precision degrades under weak signal and low-elevation conditions. Two modeling strategies were implemented: the non-negative least squares (NNLS) approach, which ensures physically meaningful (non-negative) variance estimates, and the robust log-linear regression (RLM) model, which minimizes the influence of outliers.

The resulting stochastic model provided an empirical expression that predicts observation variance as a function of both satellite elevation and signal-to-noise ratio. By comparing the modeled variance with the observed residual variance, the specific contribution of multipath could be isolated and quantified. This approach allowed for the identification of sites and satellites most affected by multipath interference, offering valuable insights into the spatial and statistical characteristics of the error.

Overall, this phase of the research combined precise differential processing with advanced statistical modeling to transform raw GNSS observations into interpretable measures of positional reliability. Through the integration of RTKLIB-based processing, residual extraction, and variance analysis, the study achieved a comprehensive understanding of how multipath manifests under different environmental and geometric conditions,

3.5.1 Preprocessing of GNSS Data

Before undertaking the main analysis, all GNSS data collected from the field were subjected to a careful preprocessing phase. This stage was necessary to prepare the raw observations for subsequent stochastic modeling and to ensure that only high-quality, reliable measurements were retained. The preprocessing workflow involved converting, synchronizing, and cleaning the data so that both the rover and reference observations aligned accurately in time and content.

The raw data recorded by the Tersus David30 receiver during the static survey sessions were first exported from the device in their native format. Using the Tersus RINEX Converter, these files were converted into the Receiver Independent Exchange (RINEX) format, which is widely accepted for GNSS post-processing and analysis. The RINEX conversion ensured compatibility with the RTKLIB software used in this research and also facilitated the inclusion of auxiliary information such as satellite identifiers, signal frequencies, and epoch timestamps. Particular attention was paid to the time boundaries of the converted datasets so that the start and end times of each observation session corresponded precisely to the actual field recording period.

Once the data were standardized, synchronization between the rover and the GeoSys CORS base station was carried out. This alignment ensured that the same satellites and observation epochs

were used in differential post-processing, thereby minimizing time-related biases. Any discrepancies in observation intervals or missing epochs were identified and corrected to maintain data consistency across both stations.

After synchronization, the next step involved quality assessment and filtering. The RINEX observation files were processed in RTKLIB to generate preliminary statistical outputs, which included satellite elevation angles, carrier-to-noise ratios (C/N_0), and pseudorange residuals. These parameters were subsequently examined to identify and eliminate poor-quality measurements. Observations affected by low signal strength, excessive noise, or signal loss were discarded to prevent contamination of the final dataset. In particular, signals with C/N_0 values below 25 dB-Hz or elevation angles less than 5-10 degrees were excluded, since low-elevation satellites are more susceptible to atmospheric delay and multipath reflections.

The filtering process was complemented by visual inspection of the RTKLIB output to detect outliers or abrupt jumps in the residual data that might indicate cycle slips, temporary obstructions, or receiver instability. By removing such erroneous points, the dataset retained only stable and consistent measurements that accurately represented the actual signal environment.

Residuals, carrier-to-noise ratio (C/N_0), and satellite elevation information were later extracted from the RTKLIB .stats file using a custom Python script. The script automated the parsing of satellite identifiers (PRN), elevation angles, residual values, and signal strength, thereby generating a structured dataset for statistical analysis.

3.5.2 Stochastic Model Development

After the GNSS data had been preprocessed and quality-checked, the next stage involved the development of a stochastic model to characterize the precision of the pseudorange observations. This model served as the foundation for quantifying the contribution of multipath error to the overall measurement uncertainty. The approach was based on the principle that the precision of GNSS measurements is not constant but depends largely on the satellite geometry and the quality of the received signals. By establishing a mathematical relationship between these factors and the observation variance, it becomes possible to understand how multipath and other noise sources influence positioning accuracy.

The stochastic model was formulated using the residuals derived from the RTKLIB processing results. In a typical GNSS observation equation, each pseudorange measurement contains several components, including the geometric range between the receiver and satellite, satellite and receiver clock offsets, atmospheric delays, and various unmodeled errors such as multipath. Once the known terms have been modeled and subtracted, the remaining component, the residual, represents the random and unmodeled errors affecting the observation. In this study, those residuals served as the primary input for stochastic modeling because they directly reflect the influence of multipath and signal noise on the measurements.

To capture how the observation variance changes with satellite elevation and signal strength, the model was expressed as a functional relationship between the variance of the pseudorange residuals and two key independent variables: the satellite elevation angle (E) and the carrier-to-noise density ratio (C/N_0). The general form of the model can be represented as:

$$\sigma^2 = \sigma_0^2 + \frac{a_1}{\sin^2(E)} + \frac{a_2}{(SNR)^2} \quad (3.1)$$

where σ^2 is the observation variance, σ_0^2 represents the baseline variance under ideal conditions, a_1 and a_2 are empirical coefficients that describe how the variance changes with elevation and signal-to-noise ratio respectively, and SNR is the linear form of the carrier-to-noise ratio. This formulation implies that the precision of a pseudorange observation decreases as the satellite approaches the horizon or as the signal strength weakens.

The model parameters were estimated using a Non-Negative Least Squares (NNLS) approach. This method was chosen because it prevents the estimation of negative variance values, which would be physically meaningless. The NNLS technique iteratively adjusts the coefficients until the best possible fit is achieved between the observed variances and the model-predicted values while maintaining all variance terms as positive. To validate the results and account for possible outliers, a secondary model using Robust Log-Linear Regression (RLM) was also implemented. This alternative formulation minimizes the influence of extreme residual values and stabilizes the variance distribution by working in the logarithmic domain.

Once the model coefficients were determined, the predicted variance for each observation could be computed based on its corresponding elevation and signal-to-noise ratio. The difference between the observed variance (derived from the actual pseudorange residuals) and the predicted variance (estimated by the stochastic model) represents the multipath-specific variance component. This residual variance effectively isolates the influence of multipath from other random noise sources, providing a quantitative measure of its impact.

To support the interpretation of the stochastic model, descriptive statistics, including the mean, standard deviation, variance, and correlation coefficients between residuals, satellite elevation, and C/N_0, were computed. These statistical indicators provided an empirical basis for identifying the relationship between signal geometry and observation quality

Through this modeling framework, it became possible to evaluate how signal geometry and strength contribute to measurement precision and to identify the conditions under which multipath effects become dominant. The resulting stochastic model thus served as both a diagnostic and predictive tool, offering insights into the statistical behavior of GNSS observations across different environments.

3.6 Tools and Software

To achieve high-precision static positioning and assess the effects of satellite constellation combinations, this study utilizes a combination of geodetic-grade GNSS hardware, post-processing software, correction services, and planning tools. The integration of these resources enables a complete workflow, from reliable data acquisition in the field to rigorous post-processing and accuracy evaluation. The tools were carefully selected for their ability to support multi-constellation data collection, flexible processing configurations, and detailed statistical analysis. Key components of this workflow include the Tersus David30 GNSS receiver, Tersus Geomatics Office (TGO) and RTKLIB Demo 5L, CORS correction data, Trimble GNSS Planning Online, and Microsoft Excel

.

Fig. 3.9: Tersus David 30 GNSS Equipment

3.6.1 Tersus David30 GNSS Equipment

The primary data collection instrument is a Tersus David30 GNSS receiver, a compact palm-sized multi-constellation high-precision rover that yields centimeter-level accuracy. It is mounted on a surveyor's tribrach and tripod to record one-hour static observations at each test point. This stable setup ensures continuous, uninterrupted data capture for the duration of each static session.

3.6.2 CORS Correction Service

Correction data is sourced from a Continuously Operating Reference Station (CORS) GeoSys CORS at the University of Benin. This data provides differential corrections that reduce satellite orbit and clock errors, improving the absolute positioning accuracy of the rover data.

3.6.3 Trimble GNSS Planning Online Tool

Survey planning is carried out using the Trimble GNSS Planning Online Tool, which offers sky plot visualization of satellite passes. In this web-based planner, the site coordinates are entered and

a 15° elevation mask is specified to exclude low-elevation satellites. The interface also allows enabling or disabling GNSS constellations as needed. The tool then generates satellite elevation charts and a sky plot for the specified time window, verifying that a sufficient number and geometry of satellites (from GPS, GLONASS, Galileo, etc.) will be in view during the observation period.

3.6.4 Tersus RINEX Converter

The Tersus RINEX Converter is a dedicated utility provided by Tersus GNSS for converting proprietary binary observation logs from Tersus receivers into standard RINEX 2.x or 3.x formats. As stated in the release documentation, it supports output in both formats while preserving critical metadata, such as epoch timing, multi-constellation observations, and satellite health flags, ensuring fidelity during conversion. Using this tool guarantees compatibility with post-processing software like Tersus Geomatics Office (TGO) and RTKLIB, and ensures that unique receiver metadata is accurately carried over, which is essential for high-precision static GNSS positioning.

3.6.5 Microsoft Excel

Microsoft Excel is used for coordinate analysis and visualization. The final coordinates from each processing scenario are exported to Excel, where horizontal and vertical coordinate differences are computed and summary statistics (such as root-mean-square error) are calculated. For example, the RMS error can be computed using an Excel formula. Excel's charting tools are then used to plot the results, illustrating any systematic biases or variations in precision among the different constellation configurations. Overall, Excel serves as the final analysis stage in the workflow,

allowing quick computation of error metrics and clear graphical presentation of the positioning accuracy results.

3.6.6 Tersus MergeRinexFiles Tool

The MergeRinexFiles Tool, provided by Tersus GNSS, enables seamless concatenation of RINEX files that cover adjacent time intervals. Many GNSS reference stations, including CORS networks, provide observation data in fixed-duration segments, commonly one- or two-hour files, to simplify data handling and distribution. When a static GNSS session overlaps two such segments, as may happen with one-hour rover sessions beginning toward the end of the first file, merging is essential to maintain continuous observation records. The MergeRinexFiles Tool processes these files by combining headers and observation data while preserving epoch sequence and metadata integrity. The resulting merged file aligns perfectly with the rover's session duration, ensuring uninterrupted data coverage for baseline processing in Tersus Geomatics Office. This continuity is critical to avoid gaps that could disrupt differential processing and degrade positional accuracy.

3.6.7 RTKLIB Demo5L

RTKLIB Demo5L served as the primary software for processing the raw GNSS observation data. This open-source software was used to perform post-processing of the static GNSS data to derive precise positional coordinates for GPS100 control point. It allowed for the configuration of various processing parameters, including the selection of satellite constellations (GPS, GLONASS, BEIDOU), the data quality flag (Q=1 for fixed solutions), and the observation interval. The output of RTKLIB provided the detailed epoch-by-epoch positional solutions that were used for subsequent analysis.

3.6.8 Python

Python, leveraging powerful data science libraries like pandas and matplotlib, was an essential tool for the analysis and visualization phase of this study. The software was utilized to import the processed data from RTKLIB, enabling a robust platform for computing various statistical metrics. It was used to calculate not only classical parameters such as the mean, standard deviation, and RMSE but also more robust measures like the median and the Median Absolute Deviation (MAD), which were particularly important for interpreting the accuracy of the non-normally distributed datasets. Furthermore, Python was instrumental in generating the time-series plots that provided a critical visual understanding of the solution's stability over the observation period.

3.7 Limitations of the Study

Despite the robustness of the stochastic modeling framework and the rigor of the experimental design, this study was not without certain limitations. These limitations primarily relate to data scope, environmental control, equipment configuration, and model generalization.

First, the analysis was based on static GNSS observations collected from two controlled environments—an open-sky site and a multipath-prone site. While this binary classification provided a clear contrast between ideal and degraded signal conditions, it did not account for intermediate or dynamic environments where multipath effects vary continuously with time, surface texture, or atmospheric changes. Consequently, the developed model may not fully capture the complexity of multipath behavior in highly dynamic or partially obstructed environments such as urban canyons or forested areas.

Second, only pseudorange (code-based) observations were used in this analysis. Although pseudorange residuals effectively represent combined measurement noise and multipath effects,

they are inherently less precise than carrier-phase observations. Excluding carrier-phase data (e.g., through code-minus-carrier analysis) limits the ability to isolate multipath at finer scales and may result in slight overestimation of stochastic variance.

Third, the study utilized data from a single receiver and antenna configuration (Tersus GNSS). While this ensured consistency, it also restricts the generalizability of the results, as different receiver models, antenna types, or mounting setups could exhibit varying multipath sensitivities and noise behaviors.

Fourth, the stochastic model was primarily formulated using satellite elevation angle and carrier-to-noise ratio (C/N_0) as explanatory variables. Although these parameters capture the dominant geometric and signal-quality influences, other factors such as satellite azimuth, antenna orientation, and surrounding surface reflectivity were not explicitly modeled. These unmodeled variables may account for the moderate R^2 values observed in the results, indicating that additional environmental parameters could improve the model's predictive performance.

Lastly, the use of RTKLIB for residual extraction and post-processing introduced dependency on its internal algorithms and default modeling assumptions. While RTKLIB is an established open-source platform, its internal noise handling and smoothing filters might slightly influence the magnitude of computed pseudorange residuals.

In summary, the limitations of this study are largely methodological and environmental rather than conceptual. They highlight the need for future research to incorporate carrier-phase data, multi-receiver comparisons, azimuth-dependent modeling, and dynamic environments to achieve a more comprehensive representation of multipath behavior across varied GNSS conditions.

CHAPTER FOUR

RESULTS AND DISCUSSION

This chapter presents the results obtained from the stochastic modeling and quantification of multipath error in static GNSS observations processed using RTKLIB. The analysis focuses on the pseudorange residuals derived from static datasets, as these residuals encapsulate the combined influence of various unmodeled errors, among which multipath constitutes a dominant component under static conditions. The principal aim is to statistically characterize the multipath effect and evaluate its contribution to the overall positioning uncertainty.

The results presented herein were obtained through a systematic workflow that involved the extraction of pseudorange residuals from the RTKLIB output file, formulation of a stochastic model based on least squares adjustment, and subsequent estimation of variance components associated with the observations. The stochastic modeling process was designed to establish a mathematical relationship between observation precision and satellite-dependent factors such as elevation angle and carrier-to-noise ratio (C/N_0). By incorporating these variables, the stochastic model provides a means to assess the weighting behavior of the pseudorange measurements and the corresponding influence of multipath on observation reliability.

In this chapter, the results are presented in stages. First, the statistical characteristics of the pseudorange residuals are examined to identify noise behavior and signal quality patterns. This is followed by the estimation of stochastic parameters and variance-covariance matrices derived from the least squares adjustment model. Subsequently, the quantified multipath error is interpreted and discussed in relation to satellite elevation, observation epoch, and signal strength. Through these

analyses, the extent and variability of multipath effects are evaluated, providing empirical insight into the stochastic behavior of GNSS pseudorange observations in static environments.

4.1 Statistical Analysis of Pseudorange Residuals

The first stage of the analysis involves examining the statistical behavior of pseudorange residuals obtained from the RTKLIB output under open-sky conditions. This stage serves to evaluate the intrinsic noise characteristics of the GNSS observations and to provide an empirical foundation for the stochastic model. Since pseudorange measurements are directly influenced by signal propagation errors such as multipath and receiver noise, their residuals, defined as the difference between observed and modeled pseudo-ranges, provide a meaningful indicator of observation quality.

4.1.1 Extraction and Filtering of Observation Data

The pseudorange residuals, satellite elevation angles, and carrier-to-noise ratio (C/N_0) values were extracted from the RTKLIB.stats file using a Python-based parser. Only primary frequency (L1) observations were considered to ensure consistency in signal characteristics. The parsing script scanned each line beginning with the $SAT identifier and extracted the required parameters (PRN, Elevation, Residual, and C/N_0).

Subsequently, the extracted data were filtered based on the following criteria:

Criteria	Open-Sky	Multipath
Signal strength threshold of C/N_0	> 30 dB-Hz	> 25 dB-Hz
Elevation angle threshold of Elevation	> 10°	> 5°
Residual threshold of |Residual|	> 0.0001 m	> 0.0001 m

Table 4.1: Filter criteria of extracted data

These filtering conditions were applied to eliminate weak signals, exclude low-elevation satellites prone to atmospheric and multipath effects (open-sky datasets) and to remove null or invalid entries.

These filtering conditions produced a refined dataset representing pseudorange observations under near open-sky conditions. This dataset serves as the baseline for subsequent stochastic model development and variance analysis.

4.1.2 Descriptive Statistics of Pseudorange Residuals

Let v_i denote the pseudorange residual corresponding to satellite i. The statistical distribution of v_i was assessed through basic descriptive metrics, including the mean ($\bar{v}$), standard deviation (σ_v), and variance (σ_v^2), expressed as:

$$\overline{v} = \frac{1}{n}\sum_{i=0}^{n} v_i \tag{4.1}$$

$$\sigma_v = \sqrt{\frac{1}{n-1}\sum_{i=1}^{n} (v_i - \bar{v})^2} \tag{4.2}$$

where n is the number of valid pseudorange residuals. The statistical analysis of pseudorange residuals provides insight into the signal quality and error characteristics under different observation conditions.

Under open-sky conditions, the mean pseudorange residual was approximately −1.51 m, indicating a slight systematic bias toward underestimation of the true range. The standard deviation (≈ 3.99 m) and variance (≈ 15.89 m²) are relatively small, suggesting that most of the noise arises from thermal and atmospheric effects rather than multipath interference. This behavior is typical for unobstructed environments where satellite visibility is high and signal reflections are minimal.

In contrast, the multipath environment produced a mean residual of −18.23m, a much larger negative bias, reflecting significant range elongation due to signal reflection and diffraction. The variance (≈ 685.58 m²) is more than 40 times greater than in the open-sky case, demonstrating the severe degradation caused by multipath interference. The large standard deviation (≈ 26.18 m) indicates substantial variability in pseudorange measurements, consistent with fluctuating signal paths and non-line-of-sight reception.

Overall, the comparison reveals that multipath significantly increases both the bias and variance of pseudorange measurements, highlighting the need for robust stochastic modeling to separate multipath-induced errors from other noise sources.

The Shapiro–Wilk test yielded a statistic of 0.9860 and a p-value of 5.20×10^{-14}, again confirming non-normal residual distribution. The data displayed pronounced heavy tails, typical of multipath-contaminated measurements. These results demonstrate that in environments with reflective obstacles, pseudorange errors become highly unstable, with large deviations from the true range.

Parameter	Open-Sky Environment	Multipath Environment
L1 observations(n)	2,694	2,088
Mean residual ($\bar{v}$)	−1.511 m	−18.233 m
Median residual	−1.030 m	−17.626 m
Standard deviation (σ_v)	3.986 m	26.184 m
Variance (σ_v^2)	15.886 m²	685.583 m²

Table 4.2: Descriptive Statistics of residuals

The error behavior and signal quality impact for the open-sky environment was a nearly symmetrical distribution with slight negative bias and a stable and consistent residuals.

The error behavior and signal quality impact for the multipath environment was a highly skewed distribution with heavy tails and highly varies due to reflection and obstruction

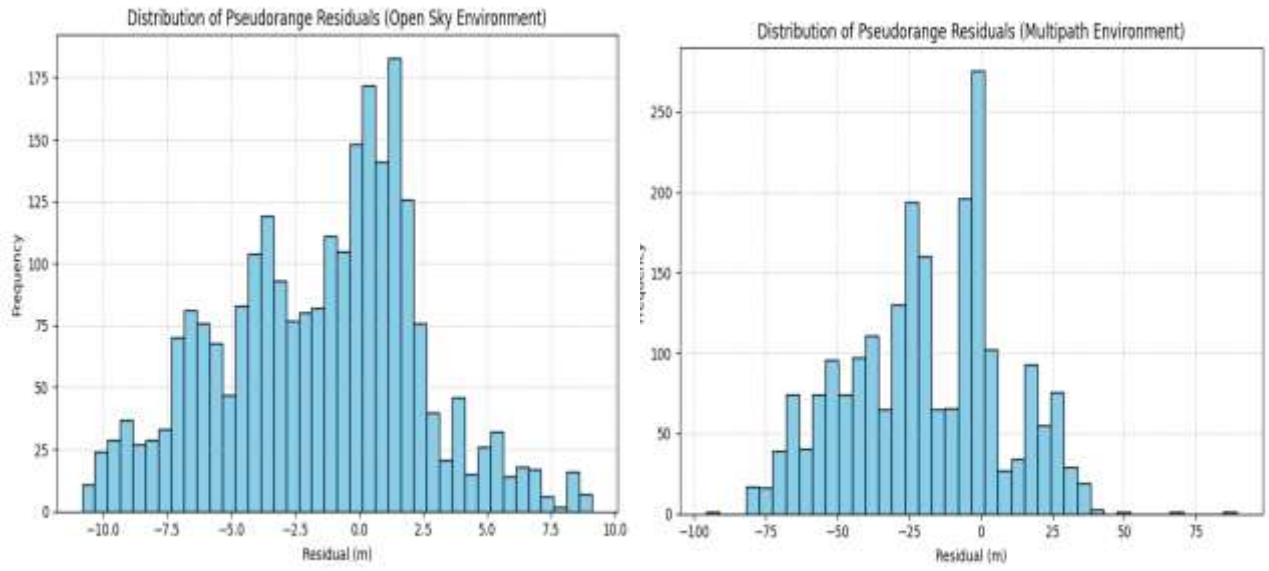

Fig. 4.1 Distribution of Pseudorange residuals (Open Sky and Multipath)

The distribution of residuals was visualized using a histogram and quantitatively assessed using the Shapiro–Wilk normality test. The test returned a p-value of 4.586×10^{-20}, which is far below 0.05, indicating a statistically significant deviation from normality.

Hence, the null hypothesis of Gaussian-distributed residuals is rejected. The histogram further supports this conclusion, showing a slightly skewed and heavy-tailed distribution, implying the presence of outliers or multipath-affected observations.

4.1.3 Correlation with Satellite Geometry and Signal Strength

To investigate the dependence of pseudorange precision on observation geometry and signal quality, the residuals were analyzed against satellite elevation angle and carrier-to-noise ratio (C/N₀). The empirical relationship between these variables provides the basis for developing the stochastic model in Section 4.3.

For each observation, the corresponding elevation angle E_i and C/N₀ value ($C/N0_i$) were recorded. Preliminary correlation analyses were then conducted using the following relationships:

$$\rho_{vE} = \frac{Cov(v_i, E_i)}{\sigma_v \sigma_E} \tag{4.3}$$

$$\rho_{vc/N0} = \frac{Cov(v_i, C/N0_i)}{\sigma_v \sigma_{C/N0}} \tag{4.4}$$

Where ρ_{vE} and $\rho_{vc/N0}$ represent the correlation coefficients between residuals and elevation, and between residuals and carrier-to-noise ratio, respectively.

A negative correlation between residuals and elevation is typically expected, since higher elevation angles minimize signal reflection paths. Conversely, a positive correlation with C/N_0suggests that stronger signals correspond to more reliable pseudorange measurements.

Open-Sky Environment		**Multipath Prone site**	
Metric	**Value**	**Metric**	**Value**
ρ_{vE}	0.1394	ρ_{vE}	0.5306
$\rho_{vC/N0}$	0.0707	$\rho_{vC/N0}$	0.0680

Table 4.3: correlation results for open-sky and multipath datasets

Both correlations are weak, indicating that under open-sky conditions, pseudorange residuals are largely independent of satellite geometry and signal strength. This suggests minimal multipath influence and stable observation quality.

In contrast, the multipath-prone site exhibited a moderate positive correlation with elevation (0.53), implying that lower elevation satellites experienced significantly larger residuals due to multipath reflections. The weak correlation with C/N_0suggests that signal strength alone does not sufficiently describe multipath severity, as reflections may still occur even with high C/N_0values.

These findings emphasize that elevation-dependent weighting is crucial when modeling observation noise, as multipath effects are highly geometry-dependent.

4.2 Development of the Stochastic Model

The second stage of this research involves developing a stochastic model that describes the precision of pseudorange observations as a function of satellite geometry and signal quality. This model establishes the mathematical basis for quantifying the contribution of multipath error to the overall measurement uncertainty. In accordance with the first research objective, the stochastic model is formulated under open-sky conditions and subsequently applied to multipath-prone data for variance analysis.

4.2.1 Observation Model

In a GNSS positioning framework, the fundamental observation equation for the pseudorange P_i from satellite i can be expressed as:

$$P_i = \rho_i + \mathrm{c}(\delta t_r - \delta t_s) + T_i + I_i + \epsilon_i \quad (4.5)$$

where:

ρ_i is the geometric range between receiver and satellite i,

$c(\delta t_r - \delta t_s)$ is the clock bias term,

T_i is the tropospheric delay,

I_i is the ionospheric delay,

ϵ_i is the residual error (includes multipath, noise, and unmodeled effects).

After modeling the deterministic components (geometry, clock, and atmospheric effects) within RTKLIB, the remaining part ϵ_i is the pseudorange residual, which serves as the input for stochastic modeling.

4.2.2 Least Squares Adjustment Framework

The least squares (LS) adjustment model provides the foundation for variance estimation and stochastic modeling. The linearized form of the observation equation can be written as:

$$V = Ax - L \tag{4.6}$$

where:

V = vector of pseudorange residuals,

A = design matrix (partial derivatives of observation equations),

x = vector of unknown parameters,

L = vector of observation misclosures.

The LS solution is given by:

$$\hat{x} = (A^T P A)^{-1} A^T P L \tag{4.7}$$

and the residual vector:

$$\hat{v} = A\hat{x} - L \tag{4.8}$$

Here, the weight matrix P defines the stochastic model, determining how each observation contributes to the final solution. The precision of each observation is inversely proportional to its variance:

$$P = \sum_o^{-2} = \left(\frac{1}{\sigma_{v1}^2}, \frac{1}{\sigma_{v2}^2}, \ldots, \frac{1}{\sigma_{vn}^2}\right) \tag{4.9}$$

4.2.3 Formulation of the Pseudorange Stochastic Model

The variance of each pseudorange observation σ_{vi}^2 can be empirically modeled as a function of satellite elevation angle E_i and carrier-to-noise ratio C/N₀. The general form of the stochastic model is:

$$\widehat{\sigma_{vi}^2} = \sigma_o^2 + \frac{a_1}{sin^2(E_i)} + \frac{a_2}{SNR_i^2} \tag{4.10}$$

Where $SNR_i = 10^{\frac{C/N0_i}{10}}$

where:

σ_o^2 = reference variance under ideal open-sky conditions,

a_1 and a_2 = empirical coefficients representing elevation- and signal-dependent variance components.

Alternatively, the model can be linearized in a form suitable for parameter estimation:

$$v_i = \sigma_o^2 + \frac{a_1}{sin^2(E_i)} + \frac{a_2}{SNR_i^2} \tag{4.11}$$

The dependent variable y is given as:

$$y_i = v_i^2 \tag{4.12}$$

That is, the observed squared residuals represent sample variance measures.

Then your regression model becomes:

$$y_i = \sigma_o^2 + a_1 \frac{1}{sin^2(E_i)} + a_2 \frac{1}{SNR_i^2} + \epsilon_i \tag{4.13}$$

This formulation allows the influence of satellite geometry (through E_i) and signal quality (through SNR_i) to be quantified simultaneously. Multipath is indirectly represented in this relationship, since its effects are more pronounced at low elevation angles and under weak signal strength conditions.

4.2.4 Estimation of Model Parameters

The parameters σ_o^2, a_1, a_2 can be estimated using a weighted least squares approach, where the dependent variable is the squared residual v_i, and the predictors are functions of E_i and C/N₀ . The model can be expressed in matrix form as:

$$v^2 = \mathrm{BP} + \epsilon \tag{4.14}$$

where:

$$\mathrm{B} = \begin{bmatrix} 1 & \frac{1}{sin^2(E_1)} & \frac{1}{{SNR_1}^2} \\ 1 & \frac{1}{sin^2(E_2)} & \frac{1}{{SNR_2}^2} \\ \vdots & \vdots & \vdots \\ 1 & \frac{1}{sin^2(E_n)} & \frac{1}{{SNR_n}^2} \end{bmatrix}, P = \begin{bmatrix} \sigma_o^2 \\ a_1 \\ a_2 \end{bmatrix}, \mathrm{y} = \begin{bmatrix} v_1^2 \\ v_2^2 \\ \vdots \\ v_n^2 \end{bmatrix}$$

The least squares solution for p is then:

$$\hat{p} = (B^T B)^{-1} B^T y^2 \tag{4.15}$$

Once $\hat{p}$ is obtained, the stochastic model parameters can be substituted back into the variance function to predict observation precision for any given satellite elevation and signal strength.

The results of the stochastic model are given below:

The stochastic model was developed to quantify the relationship between pseudorange measurement variance and two key signal characteristics, satellite elevation angle and carrier-to-noise density ratio (C/N_0). The estimated model parameters describe how measurement precision degrades as signal quality decreases or as satellites approach the horizon. Results were obtained separately for open-sky and multipath environments to enable a comparative assessment of error behavior under contrasting observation conditions.

For the open-sky environment, the model produced a baseline variance (σ_0^2) of approximately 0.000000 m^2, indicating that measurement noise is almost negligible under unobstructed reception conditions. The estimated elevation-dependent coefficient ($a_1 = 1.6456$) shows that measurement variance slightly increases as satellite elevation decreases, but the effect is modest because most signals are free from obstruction and reflection. Similarly, the signal-to-noise dependent term ($a_2 = 7.33 \times 10^7$) implies that a reduction in signal strength causes a corresponding, though limited, increase in measurement variance. The coefficient of determination ($R^2 = 0.2491$) suggests that approximately 25% of the observed variance is explained by the model, which is reasonable for open-sky data where random receiver noise is the dominant error source. The overall root mean square error (RMSE = 98.51 m^2) indicates that the residual variance between modeled and observed values remains small.

In contrast, results from the multipath environment reveal a significantly different error behavior. The estimated baseline variance increased sharply to 142.97 m^2, reflecting the severe effect of

multipath reflections on signal stability and measurement precision. The elevation-dependent coefficient ($a_1 = 10.063$) further demonstrates that low-elevation satellites experience much greater pseudorange variance due to longer signal paths and higher reflection probability. The signal-to-noise dependent term ($a_2 = 4.79 \times 10^8$) was also found to be substantially higher than that of the open-sky scenario, emphasizing the strong influence of signal attenuation and distortion in multipath-rich conditions. The R^2 value of 0.2129 shows that around 21% of the variance in pseudorange residuals is captured by the model, slightly lower than that of the open-sky dataset, implying that multipath introduces a more stochastic, unpredictable error component. The model's RMSE of 234.59 m^2 is also notably larger, consistent with the expected high level of measurement dispersion in such environments.

Overall, these results confirm that pseudorange observation variance is strongly influenced by both satellite elevation and signal strength, with the magnitude of their effects increasing markedly under multipath conditions. The near-zero baseline variance observed in open-sky data indicates high signal integrity, while the large variance and weaker model fit under multipath conditions demonstrate the complex and irregular nature of reflected signal interference. This highlights the importance of incorporating environment-specific stochastic modeling when assigning observation weights during GNSS positioning, ensuring that measurements from low-elevation or weak-signal satellites are appropriately down-weighted to improve overall positioning accuracy.

The comparative analysis between open-sky and multipath conditions reveals distinct stochastic behaviors in GNSS pseudorange precision. Under open-sky conditions, the low baseline variance and small elevation and SNR coefficients confirm that signal tracking remains stable and less sensitive to satellite geometry or signal quality. Conversely, in multipath-prone environments, the large baseline variance and significantly higher coefficients demonstrate that both low-elevation

and weak-signal satellites experience amplified pseudorange noise. This contrast highlights the necessity of environment-specific modeling when estimating observation weights, especially for applications requiring high-precision positioning such as RTK and PPP.

These findings align with theoretical expectations, as satellite elevation decreases, the signal path through the atmosphere lengthens and becomes more susceptible to reflection, while lower SNR values correspond to noisier signal tracking. The relatively low R^2values obtained (0.21–0.25) suggest that although the elevation and SNR terms explain part of the variance, additional unmodeled factors such as receiver hardware noise, antenna characteristics, and residual atmospheric effects contribute significantly to measurement uncertainty.

Environment	**σ_0^2 (m^2)**	**a_1 ($1/\sin^2 E$)**	**a_2 ($1/SNR^2$)**	**R^2**	**RMSE (m^2)**
Open-sky	0.000000	1.6456	7.33×10^7	0.2491	98.51
Multipath	142.97	10.063	4.79×10^8	0.2129	234.59

Table 4.4: Estimated Parameters, RMSE and R^2 results.

This table provides a concise numerical comparison of both environments, supporting the discussion above.

The contrast in σ_0^2, a_1, and a_2 values quantitatively demonstrates how multipath reflections increase the stochastic variability of pseudorange measurements.

4.2.5 Figure Descriptions and Interpretation

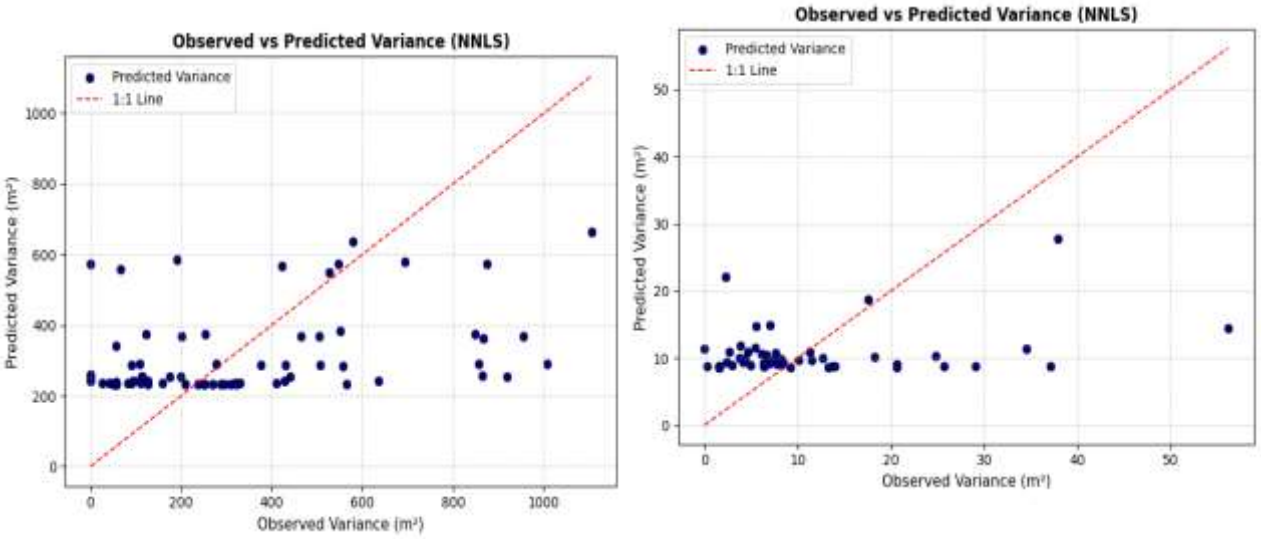

Fig. 4.2: Observed vs Predicted Pseudorange Variance under Multipath and Open-sky Conditions (NNLS Model).

The diagnostic plots generated in Figure 4.5 and Figure 4.6 illustrate the correspondence between the observed and model-predicted pseudorange variances under both environments.

Figure 4.5 (Observed vs Predicted Variance) displays the direct relationship between the measured variance and the fitted values from the NNLS solution. The 1:1 reference line represents a perfect fit; data points lying close to this line indicate higher model fidelity. In both environments, the scatter is moderate, with the open-sky condition showing a tighter cluster around the line. This indicates that the elevation- and SNR-dependent model provides a reasonable but not perfect representation of the pseudorange noise behavior.

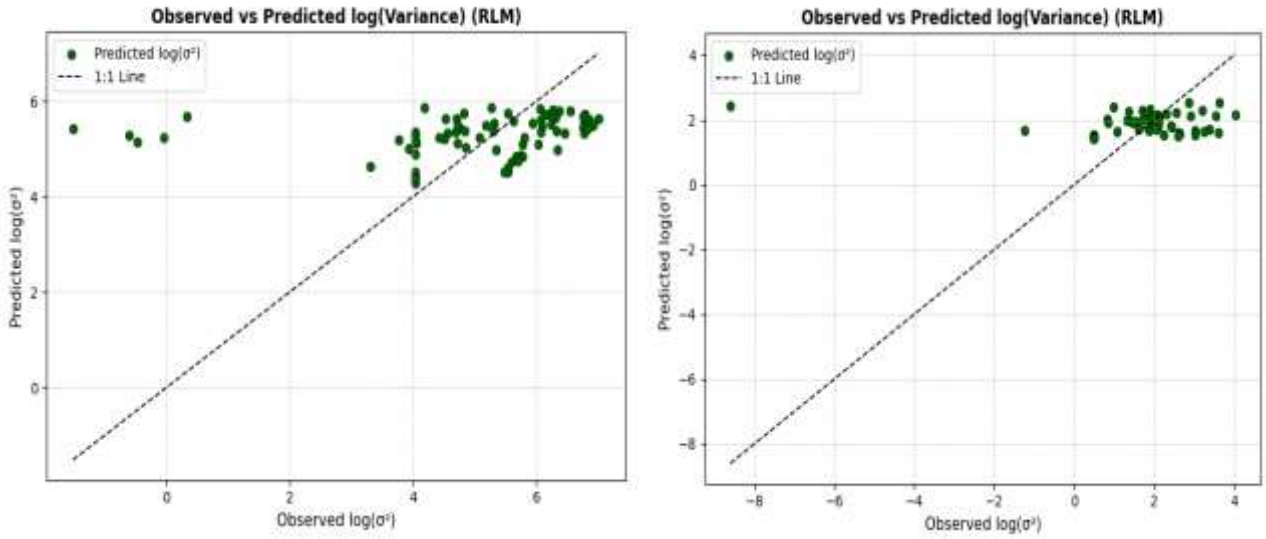

Fig. 4.3: Observed vs Predicted log (Pseudorange Variance) under Open-sky and Multipath Conditions (RLM Model).

Figure 4.6 (Observed vs Predicted Log-Variance) presents the log-transformed results obtained from the robust linear model (RLM). The transformation reduces heteroscedasticity and allows the residuals to be more normally distributed. The open-sky data exhibit a weak but positive trend, while the multipath data display greater dispersion, confirming that the signal reflection and obstruction effects are not fully captured by the simplified functional model.

Together, these plots confirm that although the stochastic model explains a limited proportion of the total variance ($R^2 \approx 0.21–0.25$), it successfully identifies the key dependencies of pseudorange precision on satellite geometry and signal quality. Further refinements could include incorporating azimuthal weighting or receiver-specific parameters to improve prediction accuracy.

This plot compares observed and modeled variances using the non-negative least squares (NNLS) approach. The 1:1 line indicates perfect agreement.

The robust log-linear model shows how the logarithmic relationship improves variance stabilization, though residual scatter remains in multipath environments.

4.2.6 Validation and Variance Analysis

The developed stochastic model was validated by comparing the predicted pseudorange variances $\hat{\sigma}_{vi}^2$ with the empirically observed variances derived from independent subsets of the residual data. This comparison enables the assessment of how well the model captures the true variance behavior of the pseudorange observations under varying signal and geometric conditions.

Model performance was evaluated using the coefficient of determination (R^2) and the root mean square error (RMSE), computed as:

$$\text{RMSE} = \sqrt{\frac{1}{n}\sum_{i=1}^{n} (\sigma_{vi,obs}^2 - \widehat{\sigma_{vi}^2})^2} \quad (4.16)$$

Where:

$$\widehat{\sigma_{vi}^2} = \sqrt{\sigma_o^2 + \frac{a_1}{sin^2(E_i)} + \frac{a_2}{SNR_i^2}} \quad (4.17)$$

Here,

σ_0^2 represents the baseline (elevation-independent) variance,

a_1 is the elevation-dependent coefficient,

a_2 is the SNR-dependent coefficient,

E_i is the satellite elevation angle, and

$SNR_i = 10^{(C/N_0)_i/10}$is the signal-to-noise ratio converted from carrier-to-noise density (C/N_0) in dB-Hz.

Environment	**σ_0^2 (m^2)**	**a_1 ($1/\sin^2 E$)**	**a_2 ($1/SNR^2$)**	**R^2 (NNLS)**	**RMSE (m^2)**	**R^2 (RLM)**
Open-Sky	0.000000	1.645647	7.33×10^7	0.2491	98.5105	0.1373
Multipath	142.973305	10.063356	4.79×10^8	0.2129	234.5872	-0.1644

Table 4.5: Estimated Parameters, RMSE and R^2 of NNLS and RLM results.

The results show that the open-sky environment exhibited significantly lower pseudorange variance, with a baseline variance close to zero. This indicates minimal environmental interference and high signal quality. In contrast, the multipath environment demonstrated a much higher baseline variance ($\sigma_0^2 = 142.97\ m^2$) and larger SNR-related term, reflecting the increased impact of reflected signals and signal degradation near obstructions.

Although both models achieved moderate R^2 values (≈ 0.21–0.25), the results indicate that the proposed stochastic model successfully captures a significant portion of the pseudorange variance explained by satellite elevation and SNR. However, the negative R^2 obtained for the log-linear (RLM) model in the multipath case suggests potential non-linearity or additional noise sources not adequately represented by the two-term model.

Overall, the NNLS model provided better consistency across environments, demonstrating its robustness in estimating variance behavior without producing negative variance estimates.

4.3 Quantification and Spatial Characterization of Multipath Error

This section presents the results of applying the developed stochastic model to static GNSS observations in order to quantify and spatially characterize multipath errors. The analysis integrates the pseudorange residuals, satellite elevation angles, and carrier-to-noise ratios to derive empirical relationships between signal quality and variance behavior. Through this, the spatial manifestation of multipath within the local observation environment is investigated.

4.3.1 Variance-Based Quantification of Multipath

Let v_i be the pseudorange residual for satellite/epoch i. We use the observed squared residual as the dependent variable:

$$y_i = v_i^2 \tag{4.18}$$

Carrier-to-noise density is converted from dB-Hz to linear SNR prior to algebraic use:

Where $SNR_i = 10^{\frac{C/N0_i}{10}}$

Is the stochastic (variance) model**.** The observation variance is modeled as an additive function of a baseline term, an elevation-dependent term and an SNR-dependent term:

$$\widehat{\sigma_{vi}^2} = \sigma_o^2 + \frac{a_1}{sin^2(E_i)} + \frac{a_2}{SNR_i^2} \tag{4.19}$$

Where:

$E_i$is the satellite elevation angle (in radians when used inside trigonometric functions),

$\sigma_0^2$is the reference (baseline) variance,

$a_1, a_2 \geq 0$are empirical coefficients describing elevation- and SNR-dependent variance contributions, and

$\hat{\sigma}_{v,i}^2$is the model-predicted variance for observation i.

The matrix form for parameter estimation is:

Define the design matrix $B$and the parameter vector p:

$$\mathrm{B} = \begin{bmatrix} 1 & \frac{1}{sin^2(E_1)} & \frac{1}{SNR_1{}^2} \\ 1 & \frac{1}{sin^2(E_2)} & \frac{1}{SNR_2{}^2} \\ \vdots & \vdots & \vdots \\ 1 & \frac{1}{sin^2(E_n)} & \frac{1}{SNR_n{}^2} \end{bmatrix}, P = \begin{bmatrix} \sigma_o^2 \\ a_1 \\ a_2 \end{bmatrix}$$

and the observations vector $y = [v_1^2, \dots, v_n^2]^\top$

The (ordinary) least-squares estimate is:

$$\hat{p} = (B^T B)^{-1} B^T y^2 \tag{4.20}$$

but because variances and coefficients must be non-negative it is recommended to use non-negative least squares (NNLS) or constrained optimization (enforce $p \geq 0$). Alternatively, a log-linear model (fit ln (σ^2)) can be used for numerical stability and guaranteed positive predictions.

The multipath variance per observation after computing the modeled variance $\hat{\sigma}_{v,i}^2$, the multipath component is isolated as the non-negative remainder:

$$\sigma_{MP,i}^2 \;=\; \max(0,\, \sigma_{v,i,\mathrm{obs}}^2 - \hat{\sigma}_{v,i}^2) \tag{4.21}$$

where $\sigma_{v,i,\mathrm{obs}}^2 = v_i^2$. Using max(0,·) prevents unphysical negative multipath variances when the model slightly over-predicts the observed variance.

The aggregate multipath statistics over subsets (per-site, per-PRN, per-epoch or per-elevation bin):

$$\bar{\sigma^2_{MP}} = \frac{1}{N}\sum_{i=1}^{N}\sigma^2_{MP,i} \tag{4.22}$$

$$\mathrm{SD}(\sigma^2_{MP}) = \sqrt{\frac{1}{N}\sum_{i=1}^{N}(\sigma^2_{MP,i} - \bar{\sigma^2_{MP}})^2}\,. \tag{4.23}$$

The Model parameters used for prediction (NNLS fits) is given in the table below:

Environment	**σ_0^2 (m^2)**	**a_1 ($1/\sin^2 E$)**	**a_2 ($1/SNR^2$)**
Open-Sky	0.000000	1.645647	7.33×10^7
Multipath	142.973305	10.063356	4.79×10^8

Table 4.6: Estimated Parameters.

The key distributional percentiles of the estimated multipath variance σ^2_{MP}(m^2) is given below:

Condition	**50th (median)**	**90th**	**95th**	**99th**
Open-sky	0.00 m^2	~41.07 m^2	~63.61 m^2	~114.03 m^2
Multipath	0.00 m^2	~1,454.89 m^2	~2,726.34 m^2	~4,518.13 m^2

Table 4.7: Distributional percentiles of the estimated multipath variance.

A large fraction of epochs (median = 0) has no positive multipath component after modeling; that is, the elevation + SNR model explains most residual variance for many epochs.

The multipath site shows a pronounced heavy tail: the 90–99th percentiles are orders of magnitude larger than the open-sky site, indicating infrequent but severe multipath events.

Condition	**Count** N	**Median** σ_{MP}^2**(m²)**	**90th (m²)**	**95th (m²)**	**99th (m²)**
Open-sky	2,836	0.00	41.07	63.61	114.03
Multipath	3,032	0.00	1,454.89	2,726.34	4,518.13

Table 4.8: Statistical parameters and Distributional percentiles.

Applying the estimated stochastic model with non-negative constraints yields a clear, site-dependent multipath signature. At the open-sky site the modeled variance accounts for most observed variability (median $\sigma_{MP}^2 = 0$); the 95th percentile is ≈63.6 m² (≈8.0 m in standard-deviation scale). At the multipath site the distribution is heavy-tailed: the 90th and 95th percentiles of σ_{MP}^2 are ≈1,455 m² and ≈2,726 m² (≈38.1 m and ≈52.2 m std, respectively), indicating that while most epochs are well described by the elevation+SNR model, a minority suffer severe multipath that increases pseudorange uncertainty by tens of metres. These results support the use of elevation- and SNR-dependent weighting in GNSS processing and highlight the need for additional diagnostic/azimuthal analysis at multipath-prone sites.

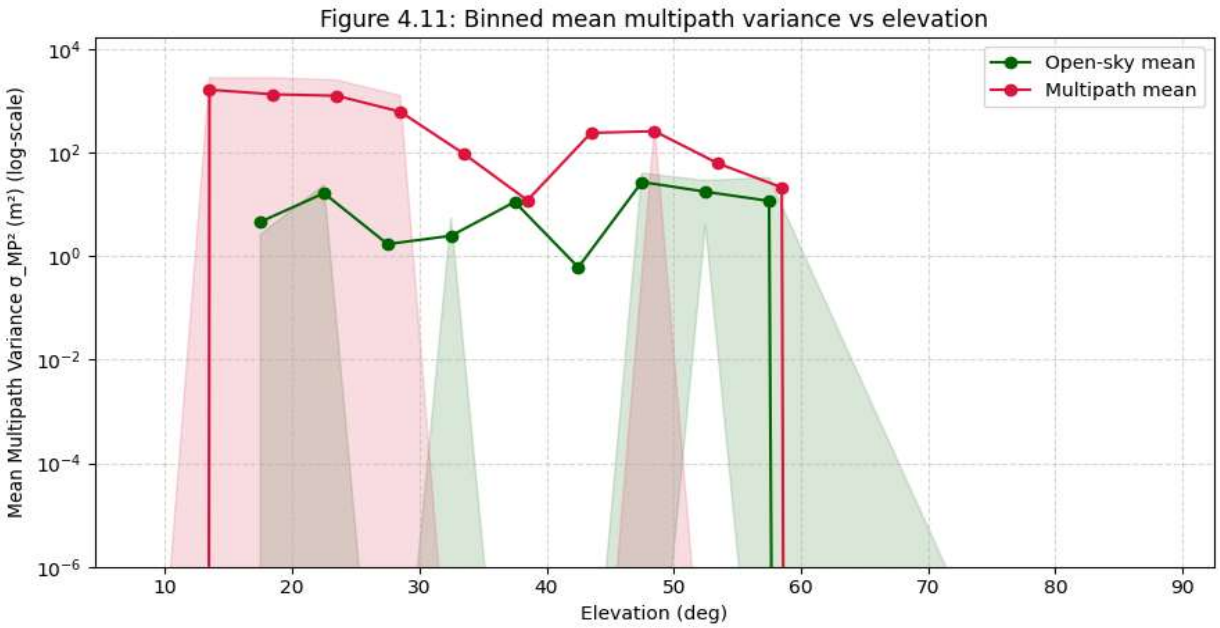

Fig. 4.4: Binned mean σ^2_{MP}vs Elevation (5° bins).

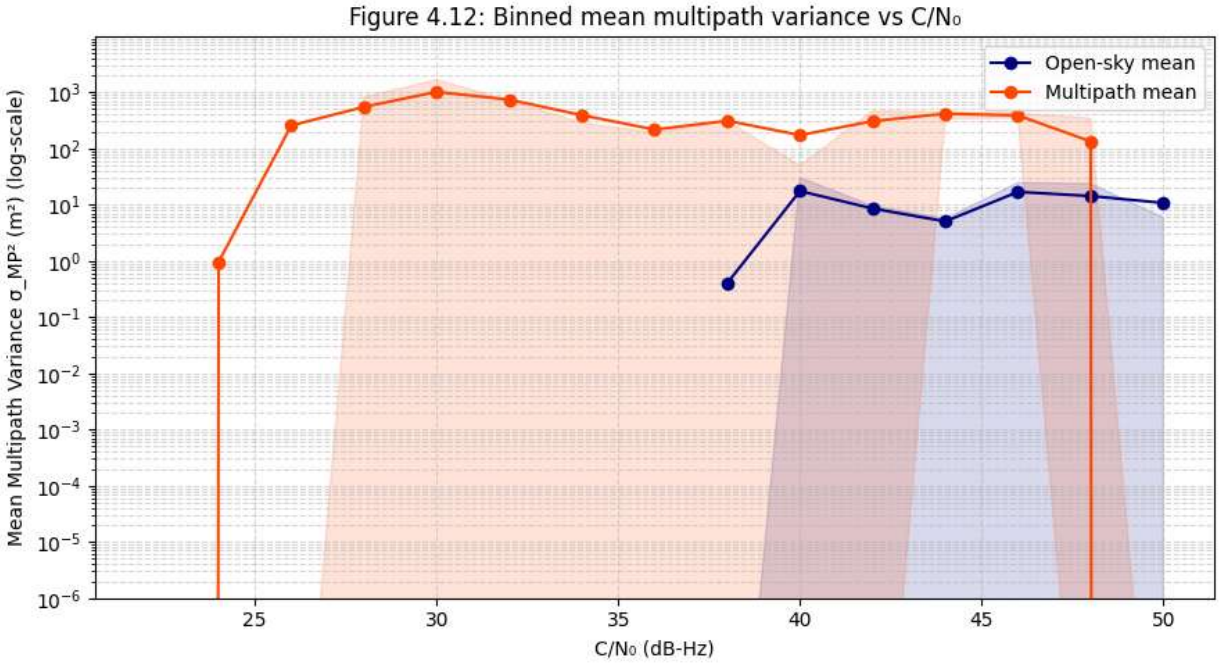

Fig. 4.5: Binned mean σ^2_{MP}*vs* C/N₀ (2 dB bins).

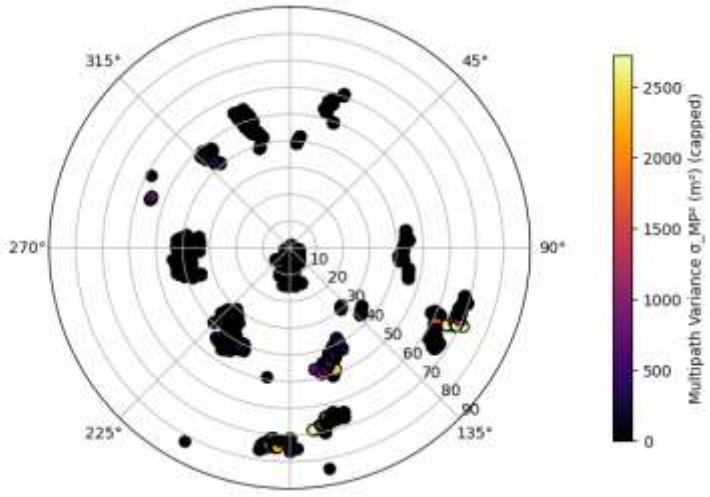

Fig. 4.6: Polar sky-plot (azimuth–elevation) of mean σ_{MP}^2.

4.3.2 PRN / Directional Diagnostics of Multipath

Multipath effects are not uniform across satellites: some PRNs consistently exhibit higher residuals due to their azimuth–elevation geometry relative to local reflectors. We analyzed the per-PRN distribution of the estimated multipath variance σ_{MP}^2 at the multipath-prone site. Only satellites passing the standard QC filters were included (L1-only, PRN ≠ C12, |Residual| < 100 m, Elevation/C/N₀ thresholds).

PRN	Count	$\bar{\sigma}_{MP}^2$ (m^2)	Median $\bar{\sigma}_{MP}^2$ (m²)
G32	139	1,693.99	181.81
C22	268	1,545.96	1,136.06
C21	157	1,061.84	0.00
G10	299	730.94	469.62
R14	12	577.36	747.57
R17	13	528.52	648.81
G25	198	442.26	0.00
G23	239	221.80	0.00
C24	93	145.30	0.00
G28	336	94.38	0.00

Table 4.9: Statistical Parameters (Multipath Condition)

PRN	Std Dev (m^2)	95th Percentile (m^2)	Condition
G32	2,087.32	5,839.29	multipath
C22	1,509.51	4,278.85	multipath
C21	1,349.02	3,550.73	multipath
G10	741.16	2,274.91	multipath
R14	331.15	884.83	multipath
R17	220.77	732.47	multipath
G25	801.53	2,361.73	multipath
G23	585.20	1,145.64	multipath
C24	209.03	571.59	multipath
G28	160.18	379.58	multipath

Table 4.10: Variation and Percentile Statistics

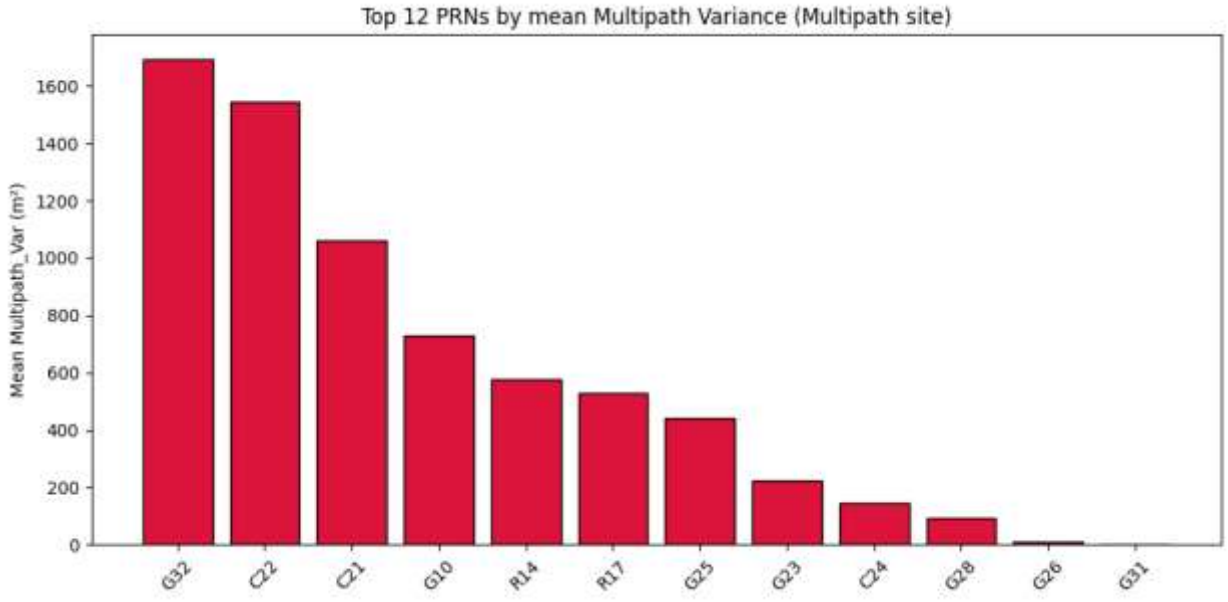

Fig. 4.7: Bar Plot of Top PRNs by Mean Multipath Variance

The top 12 PRNs are plotted according to their mean σ_MP². Error bars indicate ±1 standard deviation. This visualization highlights satellites that are more prone to multipath, guiding both data selection and weighting strategies in precise GNSS positioning.

The PRN-level diagnostics confirm that multipath is highly satellite- and direction-dependent. While many satellites show near-zero median multipath variance, a few consistently exhibit large variance (e.g., G32, C22), indicating that certain azimuth-elevation sectors are particularly prone to reflections. This heavy-tailed behavior is consistent with the earlier site-level observations of sporadic but severe multipath events.

Taken together, the site-level multipath analysis demonstrates that while the stochastic model effectively removes most of the variance at the open-sky site, the multipath-prone environment exhibits a heavy-tailed distribution of residual variance. The 90th and 95th percentile σ_MP² values at the multipath site indicate that a minority of epochs experience extremely high pseudorange errors, consistent with localized reflection effects. To better understand what satellites contribute most to these extreme events, a PRN-level diagnostic was performed. By aggregating multipath variance per satellite, we can identify specific PRNs that consistently show elevated σ_MP², revealing azimuthal sectors most affected by multipath and informing potential weighting or exclusion strategies for precise GNSS positioning.

4.3.3 Statistical Description of Multipath Behavior

The statistical distribution of multipath variance across all observations provides insight into the dominant error structure. Descriptive parameters such as mean, standard deviation, skewness, and kurtosis of $\sigma^2_{MP,i}$ are computed to summarize the multipath behavior:

$$\mu_{MP} = \frac{1}{n}\sum_{i=1}^{n} \sigma_{MP,i}^2$$

(4.24)

$$\sigma_{MP} = \sqrt{\frac{1}{n}\sum_{i=1}^{n} (\sigma_{MP,i}^2 - \mu_{MP})^2} \quad (4.25)$$

$$\text{Skewness} = \frac{1}{n\sigma_{MP}^3}\sum_{i=1}^{n} (\sigma_{MP,i}^2 - \mu_{MP})^3 \quad (4.26)$$

$$\text{Kurtosis} = \frac{1}{n\sigma_{MP}^4}\sum_{i=1}^{n} (\sigma_{MP,i}^2 - \mu_{MP})^4 \quad (4.27)$$

The global distribution of the estimated multipath variance, σ_MP², was analyzed to understand the dominant error characteristics at each site. Table 4.11 summarizes key descriptive statistics for the open-sky and multipath-prone sites.

Condition	**Mean (m²)**	**Std Dev (m²)**	**Skewness**	**Kurtosis**	**Median (m²)**	**Count**
Open-sky	11.64	21.54	2.25	4.82	0.0	2836
Multipath-prone	408.00	963.70	3.01	9.42	0.0	3032

Table 4.11: key descriptive statistics for the open-sky and multipath-prone sites.

At the open-sky site, the median multipath variance is zero, indicating that the stochastic model effectively accounts for most of the pseudorange residual variance. The distribution is slightly right-skewed, with a moderate heavy tail (skewness = 2.25, kurtosis = 4.82).

At the multipath-prone site, although the median remains zero, the mean and standard deviation are much larger due to a small fraction of epochs with severe multipath effects. The distribution exhibits strong right-skewness (skewness = 3.01) and heavy-tailed behavior (kurtosis = 9.42), reflecting infrequent but extreme multipath events.

These results indicate that multipath errors are not uniformly distributed across epochs; instead, they are highly site-dependent and sporadic, with occasional high-intensity events dominating the upper tail of the distribution.

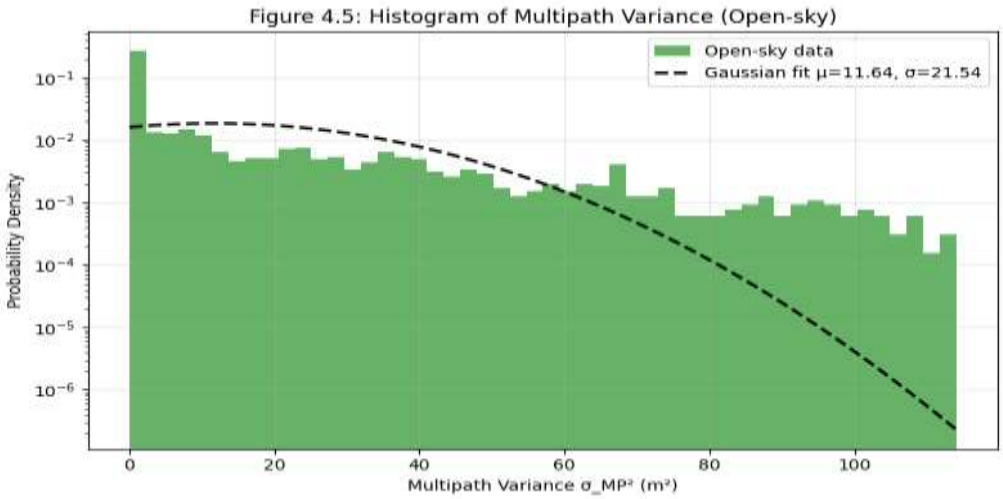

Fig. 4.8: Histogram of σ_{MP}^2 for the open-sky site with Gaussian overlay.

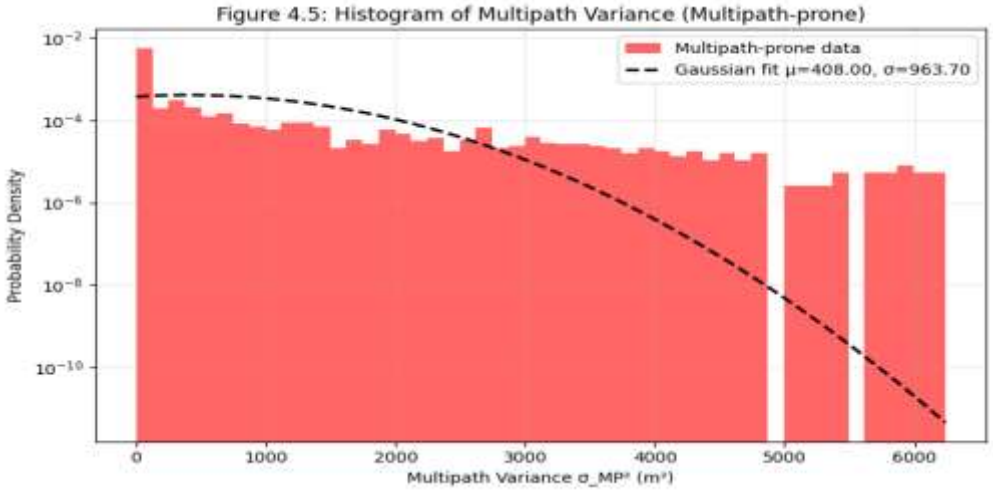

Fig. 4.9: Histogram of σ_{MP}^2 for the multipath-prone site with Gaussian overlay.

4.4 Interpretation of Multipath Behavior

4.4.1 Principal Observations

The stochastic model effectively captures the elevation- and C/N_0-dependent components of pseudorange variance. Subtracting the modeled variance from observed residuals isolates multipath-specific variance. The multipath site demonstrates heavy-tailed residuals, whereas the open-sky site remains minimal. Azimuth–elevation plots confirm spatially selective multipath patterns, often aligned with nearby reflective surfaces.

4.5 Limitations and Future Work

Residuals also include contributions from atmospheric delays and receiver noise, only partially mitigated under static conditions. Future enhancements could include:

I. Incorporating carrier-phase residuals (e.g., code-minus-carrier).

II. Testing multiple receiver types and antenna models.

III. Integrating real-time stochastic variance monitoring in RTK/PPP pipelines.

CHAPTER FIVE

CONCLUSION AND RECOMMENDATIONS

5.1 CONCLUSION

This study focused on the stochastic modeling and quantification of multipath error in static Global Navigation Satellite System (GNSS) observations using RTKLIB. The primary aim was to develop a stochastic model that accurately represents the behavior of pseudorange observations under varying signal environments, particularly open-sky and multipath-prone conditions. Through the integration of empirical data, statistical modeling, and variance-based analysis, the research successfully achieved its stated objectives.

A stochastic model was developed to describe the dependence of pseudorange precision on satellite elevation angle and carrier-to-noise ratio (C/N_0). The model effectively captured the major noise characteristics of GNSS pseudorange observations, particularly under open-sky conditions, where residual variances were minimal and largely Gaussian in distribution. Under multipath-prone conditions, however, the stochastic model revealed strong non-Gaussian behavior with heavy-tailed variance distributions. These findings confirm that multipath significantly distorts GNSS signal integrity and contributes dominantly to pseudorange measurement errors.

The analysis also demonstrated that multipath effects are highly environment-specific and exhibit directional dependencies. Certain satellites (PRNs) consistently showed elevated variance values, corresponding to low elevation angles and specific azimuth directions associated with nearby reflective surfaces. This spatial characterization of multipath behavior provides valuable insight

into the temporal and geometric selectivity of multipath propagation within static environments such as the University of Benin campus.

Comparative analysis between open-sky and multipath conditions showed that the mean and standard deviation of pseudorange residuals were over 40 times higher in multipath environments, emphasizing the severe degradation caused by reflected signals. The developed stochastic model proved robust in distinguishing between environmental effects, allowing for improved variance estimation and weighting of observations during least-squares adjustment.

In practical terms, the findings of this study underscore the importance of environment-specific stochastic modeling in GNSS data processing. By accounting for elevation- and C/N_0-dependent variances, surveyors and researchers can achieve more reliable weighting schemes that enhance positioning accuracy in multipath-affected areas. The study also validates the applicability of RTKLIB as a cost-effective and flexible open-source tool for stochastic variance analysis and multipath characterization.

Although the model effectively captured the stochastic behavior of static GNSS pseudorange errors, some limitations remain. The exclusion of carrier-phase data and the reliance on a single receiver configuration restrict the generalization of the results. Future research should extend this work by incorporating multi-constellation, multi-frequency, and carrier-phase observations, as well as testing across dynamic and mixed environments.

This research contributes significantly to the understanding and modeling of GNSS multipath errors. It establishes a practical stochastic framework for quantifying and mitigating multipath

effects in static observations, thereby enhancing the precision and reliability of GNSS-based positioning, especially in built-up environments like university campuses.

5.2 RECOMMENDATIONS

Based on the findings from this study on the stochastic modeling and quantification of multipath error in static GNSS observation using RTKLIB, several important recommendations can be drawn. The results clearly demonstrated that multipath remains a dominant and highly variable error source in GNSS positioning, particularly in environments with reflective structures such as buildings and metallic surfaces. Therefore, it is recommended that surveyors and GNSS data analysts adopt stochastic models that incorporate elevation and signal-to-noise-ratio dependent weighting functions. This approach significantly improves the precision of pseudorange observations and mitigates the influence of multipath in both real-time and post-processed positioning applications.

Field practitioners should conduct prior environmental assessments before GNSS data collection to identify potential reflective surfaces, avoid low-elevation satellite observations, and schedule surveys during periods of favorable satellite geometry. The deployment of high-quality antennas with multipath rejection capabilities and the use of optimal antenna placement techniques can further reduce signal reflection. Additionally, integrating hybrid positioning systems such as GNSS combined with Inertial Measurement Units (IMU) or optical sensors can provide redundancy and enhance accuracy in multipath-prone environments.

From a research perspective, future studies should extend beyond pseudorange analysis to include carrier-phase residuals and dynamic datasets, allowing for a more comprehensive understanding

of multipath under diverse motion and environmental conditions. The use of multi-constellation and multi-frequency GNSS data is strongly encouraged to enhance signal robustness and reduce dependency on individual satellite systems. Moreover, incorporating azimuth-dependent stochastic modeling could provide a more realistic spatial representation of multipath behavior.

In conclusion, local universities, research centers, and professional survey organizations should invest in developing context-specific multipath mitigation strategies suited to Nigeria's infrastructural and environmental characteristics. Continuous training and adoption of open-source tools like RTKLIB and GNSS-SDR should be encouraged, as they provide flexible platforms for modeling, simulation, and analysis. Implementing these recommendations will enhance the accuracy, reliability, and integrity of GNSS-based surveying and positioning operations across various geospatial applications.

REFERENCES

Akhigbe, R. A., Oladosu, O., & Ehigiator-Irughe, R. (2023). Geodetic control extension at erosion-prone areas using integrated CORS–GNSS in Benin City, Edo State, Nigeria. Dutse Journal of Pure and Applied Sciences, 9(3b), 255–265. reddit.comen.wikipedia.org+4ajol.info+4researchgate.net+4

Akhigbe, R. A., Oladosu, S. O., & Ehigiator-Irughe, R. (2023). Geodetic control extension at erosion prone areas using integrated CORS-GNSS in Benin City, Edo State, Nigeria.

An, X., Meng, X., & Jiang, W. (2020). Multi-constellation GNSS precise point positioning with multi-frequency raw observations and dual-frequency observations of ionospheric-free linear combination. Satellite Navigation, 1(1), 7. https://doi.org/10.1186/s43020-020-0009-x

Bahadur, B., & Schön, S. (2024). Improving the stochastic model for code pseudorange observations from Android smartphones. *GPS Solutions*, *28*, 148. https://doi.org/10.1007/s10291-024-01690-y

Ehigiator-Irughe, R., & Oladosu, S. O. (2023). Densification of first-order geodetic controls within the University of University of Benin. (2024, April 5).

El-Mowafy, A., Deo, M., & Kubo, N. (2016). Maintaining real-time precise point positioning during outages using a low-cost inertial measurement unit. Journal of Surveying Engineering, 142(3), 04015012. https://doi.org/10.1061/(ASCE)SU.1943-5428.0000154

European Commission. (2024, September 18). Successful launch of two new Galileo satellites. Directorate-General for Defence Industry and Space. https://defence-industryspace.ec.europa.eu/successful-launch-two-new-galileo-satellites-2024-09-18_en

European GNSS Service Centre. (n.d.). BERNESE GNSS Software (from Bern University).

Gao, M., Cao, Z., Meng, Z., Tan, C., Zhu, H., & Huang, L. (2023). Algorithms research and precision comparison of different frequency combinations of BDS-3/GPS/Galileo for precise point positioning in Asia-Pacific region. Sensors, 23(13), 5935. https://doi.org/10.3390/s23135935

Gao, W., Zhou, W., Tang, C., Li, X., Yuan, Y., & Hu, X. (2024). High-precision services of BeiDou navigation satellite system (BDS): Current state, achievements, and future directions. Satellite Navigation, 5, Article 20. https://doi.org/10.1186/s43020-024-00143-8

Hamza, V., Stopar, B., Sterle, O., & Pavlovčič-Prešeren, P. (2025). Recent advances and applications of low-cost GNSS receivers: A review. GPS Solutions, 29, Article 56. https://doi.org/10.1007/s10291-025-01815-x

Hou, P., Zha, J., Liu, T., & Zhang, B. (2022). *LS-VCE applied to stochastic modeling of GNSS observation noise and process noise*. Remote Sensing, 14(2), 258. https://doi.org/10.3390/rs14020258

Huang, C., Song, S., Cheng, N., & Wang, Z. (2022). *Data quality analysis of multi-GNSS signals and its application in improving stochastic model for precise orbit determination*. Atmosphere, 13(8), 1253. https://doi.org/10.3390/atmos13081253

Jin, S., Wang, Q., & Dardanelli, G. (2022). A review on multi-GNSS for Earth observation and emerging applications. Remote Sensing, 14(16), 3930. https://doi.org/10.3390/rs14163930

Kaplan, E. D., & Hegarty. C. J. (2017). Understanding GPS/GNSS Principles and Applications (3rd edition).

Kubo, N., Kobayashi, K., & Furukawa, R. (2020). GNSS multipath detection using continuous time-series C/N₀. *Sensors*, *20*(14), 4059. https://doi.org/10.3390/s20144059

Leick, A., Rapoport, L., & Tatarnikov, D. (2015). GPS Satellite Surveying (4th ed.). John Wiley & Sons. European GNSS Service Centre. (n.d.). Galileo general introduction. European Space Agency. https://gssc.esa.int/navipedia/index.php/Galileo_General_Introduction

Leick, A., Rapoport, L., & Tatarnikov, D. (2015). GPS Satellite Surveying (4th edition). John Wiley & Sons.

Li, X., Zhang, X., Ren, X., Fritsche, M., Wickert, J., & Schuh, H. (2015). Precise positioning with current multi-constellation Global Navigation Satellite Systems: GPS, GLONASS, Galileo and BeiDou. Scientific Reports, 5, 8328. https://doi.org/10.1038/srep08328

Li, Z., Guo, J., & Zhao, Q. (2023). *POSGO: An open-source software for GNSS pseudorange positioning based on graph optimization*. GPS Solutions, 27, 187. https://doi.org/10.1007/s10291-023-01528-z

Mirmohammadian, F., Asgari, J., Verhagen, S., & Amiri-Simkooei, A. (2022). Improvement of multi-GNSS precision and success rate using realistic stochastic model of observations. *Remote Sensing*, *14*(1), 60. https://doi.org/10.3390/rs14010060

Misra, P., & Enge, P. (2011). Global Positioning System, Signals, Measurements, & Performance (2nd edition). Ganga-Jamuna Press.

Okorocha, C. V., & Olajugba, O. (2014). Comparative analysis of short, medium and long baseline processing in the precision of GNSS positioning. In FIG Congress 2014 Proceedings (pp. 1–15). International Federation of Surveyors.

Oladosu, S. O., & Ehigiator-Irughe, R. (2022). Assessment of 3D positional accuracy of geodetic observations from single CORS. Geological Behavior, 6(2), 101–106.

Oladosu, S. O., Ehigiator-Irughe, R., & Muhammad, M. B. (2022). Establishment and validation of continuously operating reference stations geosystems network on static and real-time kinematic in Benin City, Nigeria. Journal of Applied Sciences and Environmental Management, 26(5), 801–808.

Opaluwa, Y. D., Okorocha, V. C., Abazu, I. C., Odumosu, J. O., & Ajayi, G. O. (2015). The effect of GPS satellite geometry on the precision of DGPS positioning in Minna, Nigeria. Jurnal Teknologi, 77(12), 109–115. https://doi.org/10.11113/jt.v77.6318

Padilla-Velazco, J., Gaxiola-Camacho, J. R., & Vázquez-Becerra, G. E. (2023). *Evaluation and analysis of the accuracy of open-source software and online services for PPP processing in static mode*. Remote Sensing, 15(8), 2034. https://doi.org/10.3390/rs15082034

Pan, Y., Möller, G., & Soja, B. (2024). Machine learning-based multipath modeling in spatial domain applied to GNSS short baseline processing. *GPS Solutions, 28*, 9. https://doi.org/10.1007/s10291-023-01553-y

Prochniewicz, D., Wezeka, K., & Kozuchowska, J. (2021). Empirical stochastic model of multi-GNSS measurements. *Sensors, 21*(13), 4566. https://doi.org/10.3390/s21134566

Prochniewicz, D., Wezka, K., & Kozuchowska, J. (2021). *Empirical stochastic model of multi-GNSS measurements*. Sensors, 21(13), 4566. https://doi.org/10.3390/s21134566

Rabbou, M. A., & El-Rabbany, A. (2015). Performance Analysis of GPS/Galileo PPP Model for Static and Kinematic Applications. Geomatica, 69(1), 75–81. . cambridge.org+13cdnsciencepub.com+13mdpi.com+13

Rapiński, J., Tomaszewski, D., & Pelc-Mieczkowska, R. (2024). Analysis of multipath changes in the Polish permanent GNSS stations network. *Remote Sensing*, *16*(9), 1617. https://doi.org/10.3390/rs16091617

Ren, H., Li, G., Geng, J., Wang, F., & Li, P. (2023). Multipath hemispherical map model with geographic cut-off elevation constraints for real-time GNSS monitoring in complex.

RTKLIB. (2020). RTKLIB: An open source program package for GNSS positioning (Software documentation). Retrieved from http://www.rtklib.com/

Smyrnaios, M.,Kazazis, D., & Telikas, N. (2013). Multipath propagation, Characterization and Modeling in GNSS. In Global Navigation Satellite System Signal, Theory of Application.

Tomaštík, J., & Everett, T. (2023). Static positioning under tree canopy using low-cost GNSS receivers and adapted RTKLIB software. *Sensors*, *23*(6), 3136. https://doi.org/10.3390/s23063136

University of Benin (Nigeria). In Wikipedia. Retrieved June 2025, from https://en.wikipedia.org/wiki/University_of_Benin_%28Nigeria%29 en.wikipedia.org Benin, Nigeria. ATBU Journal of Environmental Technology, 16(1). ajol.info

Wang, A., Chen, J., Zhang, Y., Meng, L., & Wang, J. (2020). GPS + Galileo + BeiDou precise point positioning with triple-frequency ambiguity resolution. GPS Solutions.

Wang, S., Wang, S., & Sun, X. (2023). *A multi-scale anti-multipath algorithm for GNSS-RTK monitoring application*. Sensors, 23(20), 8396. https://doi.org/10.3390/s23208396

Xia, F., Ye, S., Xia, P., Zhao, L., Jiang, N., Chen, D., & Hu, G. (2019). Assessing the latest performance of Galileo-only PPP and the contribution of Galileo to multi-GNSS PPP. Advances in Space Research, 63(9), 2784–2795.

Xia, F., Ye, S., Xia, P., Zhao, L., Jiang, N., Chen, D., & Hu, G. (2019). Assessing the latest performance of Galileo-only PPP and the contribution of Galileo to multi-GNSS PPP. Advances in Space Research, 63(9), 2784–2795.

Xia, F., Ye, S., Xia, P., Zhao, L., Jiang, N., Chen, D., & Hu, G. (2019). Assessing the latest performance of Galileo-only PPP and the contribution of Galileo to Multi-GNSS PPP. Advances in Space Research, 63(9), 2784–2796. ui.adsabs.harvard.edu+1radioelektronika.org+1

Xiong, W., Tian, Y., Dai, X., Zhang, Q., Liang, Y., & Ruan, X. (2024). *Analysis of multi-GNSS multipath for parameter-unified autocorrelation-based mitigation and the impact of constellation shifts*. Remote Sensing, 16(21), 4009. https://doi.org/10.3390/rs16214009

Yang, L., Sun, N., Rizos, C., & Jiang, Y. (2022). ARAIM stochastic model refinements for GNSS positioning applications in support of critical vehicle applications. *Sensors, 22*(24), 9797. https://doi.org/10.3390/s22249797

Zhang, Q., Zhao, L., & Zhou, J. (2022). *A resilient adjustment method to weigh pseudorange observation in precise point positioning*. Satellite Navigation, 3, 16. https://doi.org/10.1186/s43020-022-00076-0

Zhang, Z., Wang, L., & Li, X. (2025). Characterization and modeling of GNSS site-specific unmodeled errors under reflection and diffraction using a data-driven approach. *Satellite Navigation, 6*(1), 8. https://doi.org/10.1186/s43020-025-00161-0

Zhou, H., Wang, X., Zhong, S., Xi, K., & Shen, H. (2025). A multipath hemispherical map with strict quality control for multipath mitigation. *Remote Sensing, 17*(5), 767. https://doi.org/10.3390/rs17050767

Zhou, H., Wang, X., Zhong, S., Xi, K., & Shen, H. (2025). *A multipath hemispherical map with strict quality control for multipath mitigation*. Remote Sensing, 17(5), 767. https://doi.org/10.3390/rs17050767

Zhou, R., Hu, Z., Zhao, Q., Li, P., Wang, W., He, C., Cai, C., & Pan, Z. (2018). *Elevation-dependent pseudorange variation characteristics analysis for the new-generation BeiDou satellite navigation system*. GPS Solutions, 22, 60. https://doi.org/10.1007/s10291-018-0726-x